A MOPEVAC multivalent vaccine induces sterile protection against New World arenaviruses in non-human primates

Stéphanie Reynard, Xavier Carnec, Caroline Picard, Virginie Borges-Cardoso, Alexandra Journeaux, Mathieu Mateo, Clara Germain, Jimmy Hortion, Laure Albrecht, Emeline Perthame, et al.

A MOPEVAC multivalent vaccine induces sterile protection against New World Arenaviruses in non-human primates

Stéphanie Reynard[1,2], Xavier Carnec[1,2], Caroline Picard[1,2], Virginie Borges-Cardoso[1,2], Alexandra Journeaux[1,2], Mathieu Mateo[1,2], Clara Germain[1,2], Jimmy Hortion[1,2], Laure Albrecht[1,2], Emeline Perthame[3], Natalia Pietrosemoli[3], Audrey Vallvé[4], Stéphane Barron[4], Aurélie Duthey[4], Orianne Lacroix[4], Ophélie Jourjon[4], Marie Moroso[4], Lyne Fellmann[5], Pierre-Henri Moreau[5], Maïlys Daniau[6], Catherine Legras-Lachuer[6], Manon Dirheimer[7], Caroline Carbonnelle[4], Hervé Raoul[4], and Sylvain Baize[1,2,*]

1- Unité de Biologie des Infections Virales Emergentes, Institut Pasteur, Lyon, France.

2- CIRI, Centre International de Recherche en Infectiologie, Univ Lyon , Inserm, U1111, Université Claude Bernard Lyon 1, CNRS, UMR5308, ENS de Lyon, F-69007, Lyon, France.

3- Institut Pasteur, Université de Paris, Bioinformatics and Biostatistics Hub, Paris, F-75015, France.

4- Laboratoire P4 INSERM-Jean Mérieux , INSERM US003, 69007 Lyon, France.

5- SILABE, Université de Strasbourg, Fort Foch, 67207 Niederhausbergen, France.

6- ViroScan3D SAS, Trevoux, France.

7- INSERM, Délégation Régionale Auvergne Rhône-Alpes, Bron, France.

*Corresponding author: sylvain.baize@pasteur.fr

ABSTRACT

Pathogenic New World arenaviruses (NWAs) cause hemorrhagic fevers and can have high mortality rates, as shown in outbreaks in South America. Neutralizing antibodies (Nabs) are critical for protection from NWAs. Having shown that the MOPEVAC vaccine, based on a hyper-attenuated arenavirus, induces NAbs against Lassa fever, we hypothesized that expression of NWA glycoproteins in this platform might protect against NWAs. Cynomolgus monkeys immunized with MOPEVAC$_{MAC}$, targeting Machupo virus, prevented the lethality of this virus and induced partially NWA-cross-reactive Nabs. We then developed the pentavalent MOPEVAC$_{NEW}$ vaccine, expressing glycoproteins from all pathogenic South American NWAs. Immunization of cynomolgus monkeys with MOPEVAC$_{NEW}$ induced Nabs against five NWAs, strong innate followed by adaptive immune responses as detected by transcriptomics, and provided sterile protection against Machupo virus and the genetically distant Guanarito virus. MOPEVAC$_{NEW}$ may thus be efficient to protect against existing and, potentially, emerging NWAs.

Introduction

New World arenaviruses (NWAs) are causative agents for severe hemorrhagic fevers (HFs). Among the four clades of NWAs, clade B contains all the pathogenic strains with the exception of Whitewater Arroyo virus (WWAV), belonging to clade A/B[1]. These pathogenic strains share the same entry receptor, human transferrin receptor 1[2]. Pathogenic NWAs are a public health concern, with Junin virus (JUNV) being endemic in Argentina and having caused hundreds of cases each year before the Candid#1 vaccine was introduced[3,4]. However, this vaccine is not FDA-approved and induces adverse effects[5–7]. Machupo virus (MACV) recently re-emerged and caused hundreds of cases[8,9]. Consequently, vaccine approaches have been proposed[10,11]. The three other pathogenic NWAs, Sabia virus (SABV), Guanarito virus (GTOV), and Chapare virus (CHAV) have so far emerged only sporadically [12–14]. The evolution of rodent populations, the natural reservoir for NWAs, has been associated with human incidence[15–17]. Depending on the weather, increase in rodent populations can occur and cause viral emergence. The absence of treatment or prophylaxis for all the NWAs exposes populations to sporadic viral circulation. Moreover, new pathogenic arenaviruses regularly emerge, such as WWAV in 1999/2000[18,19], CHAV[14] in 2003/2004, and Lujo virus[20] in 2008.

Treatment of JUNV-infected patients with convalescent plasma is efficient during acute disease[21]. However, late onset encephalitis with high lethality has been reported in animal models [22,23], suggesting that this approach can control acute infection but fails to prevent viral persistence at immunologically privileged sites. Nevertheless, neutralizing antibodies (NAbs) are crucial for the control of NWAs[21,22,24]. We previously developed MOPEVAC, a hyper-attenuated Mopeia virus (MOPV)-based vaccine platform, and showed its efficacy against the Old World arenavirus Lassa virus (LASV) in macaques[25,26]. MOPEVAC$_{LAS}$ induced a T-cell response, crucial in counteracting LASV infection, as well as a robust antibody response[26].

We thus hypothesized that MOPEVAC, which induces Nabs, could protect against NWAs. We first developed $MOPEVAC_{MAC}$[25], the MOPEVAC platform expressing MACV glycoproteins. Vaccinated animals developed an antibody response with Nabs and were protected against a lethal challenge with MACV. Then, we developed $MOPEVAC_{NEW}$, a pentavalent vaccine expressing epitopes from all five pathogenic NWAs known in South America. Immunized animals produced antibodies against the five antigens and they were protected against a challenge with MACV and the phylogenetically distant GTOV. This vaccine could provide a means of preemptively protecting against the re-emergence of known NWAs**.**

Main text

MOPEVAC$_{MAC}$ induces MACV-specific antibody responses

Cynomolgus monkeys (CMs) received MOPEVAC$_{MAC}$ vaccine with a single dose (n=4) or a prime-boost strategy (n=4). Three CMs received the excipient. All were challenged with MACV (Fig. 1a).

MOPEVAC$_{MAC}$ comprises a hyper-attenuated MOPV expressing MACV glycoproteins. Activity of the exonuclease virulence factor was abolished by six mutations in the nucleoprotein[25,27–30], ensuring attenuation of MOPV, already known to be nonpathogenic (Fig. 1b). Infection of antigen presenting cells with MOPEVAC results in immune activation and in the lack of viral replication. We previously showed that we can swap the gene encoding for glycoproteins (GPC gene) with any GPC gene from arenaviruses[25]. Here, we demonstrated that equal amounts of glycoproteins were expressed in infected cells by the different MOPEVAC expressing the NWAs glycoproteins. The ratio between RNA amounts of GPC at day 3 *versus* day 0 was similar for all MOPEVAC (Extended data Fig. 1a). Similar amounts of GP2 protein were contained in all MOPEVAC viruses, except for SABV whose GP2 was not recognized by our antibodies (Extended data Fig. 1b). The replication of MOPEVAC was tested with different NWA GPC. They all replicated equally and were stable over multiple passages (fig. 1c), as previously shown for some candidates[25]. We sequenced the viruses at passage 2, 5 and 10 to confirm the absence of major changes in the consensus genome sequence after passages. No mutation was consistently present in all GPC sequences after ten passages, or in the 6 amino acids mutated to abrogate the exonuclease domain (Supp. Table 1). Only one or two amino acid changes were observed in the genome in vaccine candidates but without consequence for replication. These results confirm the stability of all MOPEVAC$_{NEW}$ components over multiple passages and in particular of the immunogenic antigen and of the attenuation phenotype.

MOPEVAC$_{MAC}$ did not induce any appreciable adverse effect *in vivo*. We never detected vaccine shedding: no MOPEVAC RNA was found in plasma, urine, or nasal and oral swabs. We detected MACV-specific IgG from day 9 post-immunization and the antibody titers rose to 1,000 during the first month (fig. 1d). The boost resulted in a rapid increase in antibody release, with titers reaching 16,000, the upper limit of our test. By day 14 after the first injection, 6 of 8 animals showed NAbs, mainly at low titers. By day 30, all animals were positive. The second vaccine injection resulted in neutralizing titers of 100 in all animals. Thus, MOPEVAC$_{MAC}$ promotes a NAb response.

MOPEVAC$_{MAC}$ induces sterile protection against MACV

After the immunization period, all animals were challenged with MACV. A clinical score was calculated each day based on the symptoms observed (Supp. Table 2). This score remained low throughout the experiment for vaccinated animals, with no difference between the vaccination regimens. Unvaccinated animals experienced fever from days 4 to 5 (Extended data Fig. 2) and from day 8, they presented with balance disorders, dehydration, and reduced interactions. They eventually reached the ethical endpoint between days 11 and 13 because of the absence of reactivity, intense dehydration, and epistaxis. They continuously lost weight from day 4 (fig. 2a), and experienced profound lymphopenia and thrombocytopenia, with a drop in hemoglobin concentration observed for 2/3 animals (Extended data Fig. 3a). They also presented increasing levels of alanine aminotransferase (ALT), aspartate aminotransferase (AST) and plasma urea, and a decrease in plasma albumin concentrations (Fig. 2b), suggesting liver and tissue damage, as well as renal injury. No alterations in hematological and biochemical parameters were detected in the vaccinated animals.

Control animals presented increasing titers of MACV from day 6 after infection in plasma and oral/nasal swabs (Fig. 2c). At the day of euthanasia, the infection was pantropic, all the organs tested were MACV-positive (Extended data Fig. 3b). However, we never detected viral RNA in any of the samples of the

vaccinated animals, neither in the fluids nor in the organs. Vaccination, even with a single dose, was able to control MACV replication. Thus, MOPEVAC$_{MAC}$ induces a sterilizing immunity in CMs.

In the vaccinated animals, we did not observe any increase in IgG titers after challenge (Fig. 2d). To ensure that a low increase in antibody levels did not occur, we represented the optical density at a single dilution. A slight decrease occurred for the prime boost group but did not alter the IgG titer and the values remained stable for prime only group. However, NAb levels increased after challenge. The titer was finally at 100 for all vaccinated animals with no heterogeneity depending on the vaccination regimen. In the control animals, specific antibodies were never detected.

We determined whether MOPEVAC$_{MAC}$ could cross-neutralize other NWAs by assaying plasma samples from the immunization period for their ability to neutralize MOPEVAC$_{JUN,GTO,CHA}$: MOPEVAC expressing respectively JUNV, GTOV and CHAV glycoproteins. Although all plasma samples presented detectable NAbs against MACV at the end of the prime period, this was not true with other NWAs (Fig. 2e). The boost injection resulted in an increase in cross-reactive NAbs except for in one animal that did not neutralize GTOV. Although titers were lower than for the homologous virus, MOPEVAC$_{MAC}$ induced cross-neutralizing antibodies.

MOPEVAC$_{NEW}$ induces antibody responses against five NWAs

Given the efficacy of MOPEVAC$_{MAC}$, we considered the generation of a multivalent vaccine protecting against all five pathogenic South American arenaviruses. This pentavalent vaccine, named MOPEVAC$_{NEW}$, includes five MOPEVAC vaccines, each expressing MACV, GTOV, CHAV, SABV, or JUNV GPC.

We vaccinated six CMs with MOPEVAC$_{NEW}$ in a prime-boost protocol, and six other animals received the vehicle (Fig. 3a). We did not observe any clinical signs during the immunization period (Extended data Fig. 4a). We also failed to detect vaccine shedding in the days following the injections (until day 9 after prime and day 5 after boost). The neutralizing titers of plasma samples were heterogeneous depending on the

MOPEVAC viruses targeted (fig. 3b). Some plasma samples did not neutralize all viruses at the end of the prime period. This result could be explained by higher detection cut-off for this experiment compared to that in the $MOPEVAC_{MAC}$ experiments. NAbs against all viruses were finally detectable in all animals after the boost with the strongest response detected against JUNV.

The kinetics of these antibody responses were similar to that observed with $MOPEVAC_{MAC}$. Vaccinated animals produced IgG against MACV and GTOV, with a strong increase observed after the boost. However, one animal from each control group presented low Ab levels at the end of the immunization period (Fig. 3c). We did not observe vaccine shedding and vaccinated CMs were not in contact with the controls. This result is therefore probably due to cellular contents present in the mock vaccine and also present in antigen preparations. To check for the presence of antibodies against other NWAs, we incubated plasma samples with 293T cells expressing GPCs. Despite differences in the level of recognition, only plasma from the vaccinated animals recognized NWA GPCs. There was no cross-reactivity with MOPV GPC (Fig 3c, Extended data Fig.5).

$MOPEVAC_{NEW}$ induces sterile protection against MACV and GTOV

Three vaccinated and three control animals were each challenged with either MACV or GTOV. MACV and GTOV infection induced illness in control animals (Fig. 4a). The evolution of the disease after MACV infection was highly similar to that of the first experiment. Animals reached the ethical endpoint between days 12 and 18. One was euthanized despite a clinical score of 13, due to a weight loss of 27%. GTOV infection induced symptoms two days later, including reduced activity, gastrointestinal symptoms, weight loss, and fever (Extended data Fig. 4b). One GTOV-control animal reached the endpoint on day 14 (Fig. 4a). The two remaining CMs presented maximum scores of 12 and 13 at day 16. These scores then decreased and by day 29, were at 10 and 5, respectively. This latter animal presented with a weight loss of 22%, which should have been an endpoint (Fig. 4a). None of the vaccinated CMs experienced clinical signs; the low

score observed was due to diarrhea, which was also observed for certain animals before the challenge and probably unspecific.

The three MACV infected controls presented viral replication in fluids and in the organs highly similar to that observed in the first experiment (Fig. 4b, Extended data Fig. 6a). GTOV-infected controls presented lower infectious titers in the fluids but high viral RNA loads (fig. 4b). Viral RNA was also measured in the organs of the deceased GTOV control but at lower titers. Infectious particles were detected mainly in the secondary lymphoid organs, the liver, the ovaries and the intestine (Extended data Fig. 6a). At the end of the protocol, the healthiest remaining GTOV-control presented the lowest viral titers in the fluids and organs. The other presented viral RNA in many organs but infectious particles were found only in the adrenal gland. We detected viral RNA in all cerebrospinal fluids (CSF) from control animals at the peak of the disease but only two MACV-infected animals had infectious particles (Extended data Fig. 6b). This indicates that the virus can cross the blood-brain barrier. The vitreous humor contained viral RNA in one surviving GTOV-infected control. We never detected viral RNA in the organs or fluids of vaccinated animals, showing that the vaccine induced a sterilizing immunity as observed with MOPEVAC$_{MAC}$. Moreover, no significant change was observed in vaccinated animals for hematological and biochemical parameters, unlike control animals (Extended data Fig. 7 a and b, respectively).

The IgG titers against GTOV increased after challenge for vaccinated animals and eventually reached the IgG titer measured against MACV (Fig. 5a). Two out of the three MACV-infected control animals had developed specific IgG by their respective endpoints (day 12 and 18). The GTOV-infected controls that survived showed increasing antibody levels from day 16. The vaccinated CMs boosted the production of NAbs specific of the virus used for their challenge (fig. 5b). We did not observe any NAbs in MACV-infected controls but all GTOV-infected controls showed significant levels of Nabs at day 12. In one of the animals that survived, the titer rose to 2,000, the highest titer measured. Unexpectedly, one of the MACV-controls

showed a low NAb titer against MOPEVAC$_{CHA}$ and $_{SAB}$, but not against wild-type MACV (Fig. 5c). As we used whole viruses for the experiments, this must have increased the risk of nonspecific neutralization.

Immune responses involved in protection

We evaluated the expression profiles of genes related to innate, T-cell and B-cell responses using a transcriptomic analysis on PBMCs from the MOPEVAC$_{MAC}$ experiment[31]. Control animals were included, with day 30 samples, the day of the second vehicle injection. After immunization, we observed strong and transient activation of the innate immune response in the first two days. The boost reactivated the response to a lower extent, before significant downregulation from day 5 (Fig. 6a, Supp. Table 3). The T-cell response was also upregulated in a very significant manner from days 4 and 5 after the prime, and from day 2 after the boost. The boost was therefore efficient in reactivating the T-cell immune response. At the day 0 timepoints, expression of B-cell response-related genes implicated was heterogeneous, including for controls, but the mean of expression in the pathway was comparable. Expression of genes related to B-cell response was quickly and significantly downregulated from day 2 after vaccination until day 9 after the prime or day 5 after the boost.

We looked for the presence of circulating MACV-specific T cells. After immunization, we stimulated PBMCs with overlapping peptides from NP and GP proteins. Super-antigen staphylococcal enterotoxin A (SEA) was used as a positive control. This stimulation did not activate expression of CD154 or CD137, markers of CD4 and CD8 T cell activation respectively, and of IFNγ, or GrzB (indicators of cytotoxic response), in contrast to the strong activation induced by SEA (Extended data Fig. 8 and 9a). After challenge, we only observed, following whole blood stimulation, a slight expression of IFNγ around day 15 in only one over 8 animals (Extended data Fig. 9b).

Transcriptomic analysis on PBMCs after challenge showed a strong and early innate immune response in control animals, which lasted until the end of the experiment. The T-cell response was downregulated until

day 6, and upregulated from day 9, in the very last days of the illness. The B-cell response was increasingly downregulated during the course of the disease (Fig. 6b, Supp. Table 3).). The day 0 was highly similar to that of the point taken during immunization period. For the vaccinated animals, we observed only a modest regulation of these pathways, more significant in the prime only group.

Discussion

Despite currently low incidence of human cases, NWAs are of concern due to the risk of emergence and the severity of the disease[32]. Immunization with the JUNV Candid#1 vaccine enabled the endemic virus to be efficiently controlled. There are also vaccines for MACV[10,11,33] at the preclinical stage. Here, we provide a vaccine candidate validated in a non-human primate model able to confer sterile protection against two distant viruses and induce NAbs against all pathogenic South American NWAs. Bivalent vaccines were previously tested but failed to provide sterile protection against different viruses[10,33]. Moreover, a study of NAbs in the plasma of Candid#1 vaccinated patients showed that there was no cross-neutralization with other NWA[34]. Yet, both known and unknown arenaviruses present a high risk of emergence or re-emergence. For example, WWAV and CHAV emerged in the last decades, while MACV, first described in the 60's after being responsible for 637 cases[35], caused sporadic cases until 2006, and re-emerged to cause more than 200 cases in 2008. CHAV also caused an outbreak in 2019[36] and GTOV in 2021[37]. Despite the quite low incidence of human contaminations, cases of human-to-human transmission were documented, mainly to health care workers and laboratory staff[35,36,38]. The recent Ebola virus epidemics and SARS-CoV-2 pandemic have shown the importance of preparedness and, concerning vaccines, the necessity of having products fully validated at the preclinical level and ready to go into the clinic. During the 2014-2016 Ebola outbreak, the use of Ervebo® vaccine helped to control the outbreak and accelerated licensing of the vaccine[39]. The low incidence of individual NWAs favors development of an easy to produce, affordable multivalent vaccine. The production of MOPEVAC$_{NEW,}$ composed of five attenuated viruses, represents a challenge, but all viruses replicate similarly and optimization of the production could provide an efficient method suitable for all five viruses. Eventually, this vaccine could protect the entire South American continent against NWAs.

We demonstrated that MOPEVAC could protect against NWAs. We were able to fully protect CMs against MACV and GTOV infection, whereas in the LASV experiment, 3/4 CMs experienced fever and low transient replication of the virus after challenge[26]. NAbs are crucial in protection against NWAs[21,22,24], the induction of NAbs following immunization met our expectations. We did not find persistent virus in any of the organs or samples tested, suggesting that the late onset encephalitis should not occur with MOPEVAC. As we detected low neutralizing titers against heterologous viruses after $MOPEVAC_{MAC}$ immunization, we created a multivalent vaccine against all known NWAs from South America. $MOPEVAC_{NEW}$ was efficient against two phylogenetically distant NWAs. Thus, we do not face low specificity and inefficient cross-neutralization as sometimes observed with multivalent vaccines.

We observed cross-neutralization between NWAs. Plasma samples from MACV-immunized CMs partially neutralized other NWAs GPCs. Interestingly, such broad NAbs are not always induced after NWA immunization[34,40]. Studies have demonstrated that NAbs against NWAs did not share the same binding site. JUNV-NAbs mainly used transferrin receptor mimicry while MACV-NAbs did not. However, NAbs able to neutralize both JUNV and MACV were found in plasma from Candid#1 vaccinated donor[41], a conserved domain in the receptor-binding site was identified. Cross-neutralization observed in MACV-vaccinated animals may thus be due to such antibodies. The $MOPEVAC_{NEW}$ vaccine expresses GPs from all NWAs and thus induced many NAbs. We observed an increase in NAb titers specifically against the virus used for the challenge. This suggests that a pool of NAbs is induced and that the infection boosts the synthesis of NAbs that are the most specific for the challenge virus. NAbs therefore seem important for protection although this was not mechanistically shown.

The immune responses promoted after immunization and challenge were different from those observed with $MOPEVAC_{LAS}$[26]. We did not detect the activation of T cells after peptide stimulation, suggesting that the vaccine did not predominantly induce a Th1 response and/or cytotoxic T cells like $MOPEVAC_{LAS}$[26]. This difference is unlikely to be due to a change in primary target cells, since both NWAs and LASV, target

antigen-presenting cells. However, the GPC carried by MOPEVAC could affect the response. Indeed, previous studies have linked the presence of N-glycans on GP1 to low neutralization capacity of NAbs[42]. Interestingly, JUNV is the most efficiently neutralized virus and its GP1 is the least glycosylated[42,43].

Transcriptomic analysis of PBMCs showed that both vaccination and infection of control animals are responsible for a strong IFN response, which is consistent with *in vitro* and *in vivo* studies[44–46]. Double-stranded RNAs (dsRNA) accumulate in NWA-infected cells and thus activate RIG-I like receptors[47]. In MOPEVAC, the mutations in the exonuclease domain prevent dsRNA degradation. Consistently, both immunization and challenge induce the overexpression of genes implicated in RIG-I like receptor signaling: *IFIH1* (MDA5), *DDX58* (RIG-I), *DHX58* (LGP2) and *DDX60*. *TLR7*, involved in single stranded RNA recognition, was upregulated after challenge. Overall, upregulation of *MX1* and *MX2* genes involved in IFN signaling is observed. After immunization, a significant T-cell response took place from day 4 and was reactivated quickly after the boost injection. Interferon-γ, TNFα, Granzyme B and perforin gene expression did not appear to be significantly regulated, reinforcing the hypothesis of a non-cytotoxic T-cell response. The genes associated with B-cell responses were significantly downregulated in the first days after vaccination. This could be due to the recruitment of B cells to the germinal centers to promote Ag recognition and initiation of the humoral response. The observed T-cell response, associated with B-cell regulation, suggests the induction of a humoral response dependent on T helper cells. This results in the strong induction of antibodies and provides protection with sterilizing immunity. NAbs were previously used as a treatment and succeeded in resolving the acute phase of the disease[21,22,24]. Here, the presence of NAbs at the time of infection may enable viral elimination before dissemination, particularly into the brain, avoiding the risk of late onset encephalitis.

MOPEVAC$_{NEW}$ is an efficacious vaccine against MACV and GTOV, two distinct arenaviruses. We detected cross-reactive NAbs produced in response to MOPEVAC$_{MAC}$ and NAbs against all NWAs tested in response to MOPEVAC$_{NEW}$. Thus, this vaccine could protect against all NWAs, including some that have still not

292 emerged. We demonstrated that this vaccine is safe. Completion of preclinical and clinical development
293 could provide a ready-to-use solution for a future emergence.

294

Methods

Study design

For the first experiment, 11 male CMs (*Macaca fascicularis*) were injected with vehicle or vaccine. The animals were 2.5 years old and weighed 2.3 to 3.9 kg. There were no significant differences in these parameters between the groups. Immunization was performed in a BSL2 animal facility (SILABE, France). Three animals received the vehicle and four animals received $MOPEVAC_{MAC}$ 67 and 37 days before challenge (controls and Prime/boost group respectively). The four remaining animals received a single dose of $MOPEVAC_{MAC}$ 37 days before challenge (Prime only group). The vaccine consisted of 2×10^6 ffu injected intramuscularly. Blood, urine, and oral and nasal swabs were sampled periodically.

Animals were challenged in the BSL4 laboratory (P4 Jean Mérieux-INSERM, Lyon, France) after 10 days of acclimation. They all received 3,000 ffu of MACV (strain Carvallo) subcutaneously. Samples were taken every two days until day 6, every three days from day 6 to day 18, and on day 22. Each sampling was performed under anesthesia (Zoletil 100, 0.1 ml/kg). Each day, the state of the animals was evaluated, and a clinical score was calculated based on behavior, body temperature, dehydration, weight loss, clinical signs, and reactivity. A clinical score ≥ 15 or weight loss > 20% were defined as an endpoint in the protocol and the animal was euthanized. The end of the protocol was planned for days 28/29. Euthanasia was performed under anesthesia with a 5 ml intracardiac injection of Dolethal or Euthasol and samples then taken as for previous sampling and the organs collected.

Animals were implanted with intraperitoneal body temperature recording systems (EMKA technologies) before the beginning of the experimentation. However, most were defective. We implanted new subcutaneous systems before the challenge (Star Oddi) but also experienced a number of issues and could finally obtain the temperature recording after challenge for only seven animals (3 controls, 3 prime only,

and 1 prime/boost). Moreover, the new implantation resulted in local inflammation that was still present for some animals at the day of challenge.

The second experiment was conducted in the same laboratories using similar protocols and procedures. The body temperature was efficiently recorded throughout the procedure using intraperitoneal loggers (Star Oddi). Twelve female CMs were used. They were almost three years of age and weighed 2.5 to 3.4 kg. Six received the vehicle and six were vaccinated with $MOPEVAC_{NEW}$ (2.10^6 ffu i.e 4.10^5 ffu of each valence). The immunization was performed on days 0 and 56. The animals were transferred to the BSL4 laboratory on day 89. After a period of acclimation of 10 days, they were challenged with an expected dose of 3,000 ffu. We titered the virus dilution used for challenge and it was actually 4,500 ffu for MACV and 3,000 ffu for GTOV. Six animals were inoculated with each virus: three vaccinated and three unvaccinated. The sampling interval was extended due to the lower weight of the animals.

Ethical statements

The protocol of the first experiment was approved by the "Comité Régional d'Ethique en Matière d'Expérimentation Animale de Strasbourg" for the immunization period and registered with the number APAFIS#18970-2019020616112503 v8 (2019/07/23) and by the ethical committee "CELYNE" (Lyon, France) for the challenge procedure and registered with the number APAFIS#18397_2019011010351235_v4 (2019/03/15).

The protocol of the second experiment was approved by the same ethical committees and registered with the numbers: APAFIS#18970-2019020616112503 v8 (2019/07/23) for the immunization protocol and APAFIS#28798_2020122311384240_v2 (2021/02/11) for the challenge procedure.

Cell lines

VeroE6 cells and 293T cells were used in this study, from ATCC (CRL-1586 and CRL-3216 respectively).

Viruses

The MOPEVAC platform consists of a MOPV (strain AN21366; GenBank accession numbers JN561684 and JN561685) that carries the GPC of the virus of interest in place of its own GPC and is mutated in the NP gene to abolish the exonuclease function[25]. The resulting attenuated virus was produced in VeroE6 cells cultivated in DMEM, 2% FCS. MOPEVAC$_{MACV}$ was then concentrated by centrifugation in filter tubes with a 1,000 kDa cutoff. A vehicle solution was prepared with uninfected VeroE6 supernatant under the same conditions and was used in the control animals in place of the vaccine injection.

MOPEVAC$_{NEW}$ is a mixture of equivalent quantities of infectious particles of MOPEVAC expressing the GPC of MACV (strain Carvallo; GenBank accession number AY619643), GTOV (strain INH95551; GenBank accession number AY129247), CHAV (strain 810419; GenBank accession number NC_010562), SABV (strain SPH114202; GenBank accession number NC_006317), and JUNV (strain P2045; GenBank accession number DQ854733). It was produced under the same conditions, except for the concentration method. The cell supernatant was precipitated using a PEG solution (Abcam). After overnight incubation at 4°C with gentle agitation, it was centrifuged for 3 h at 4,696 x g and the pellet was resuspended in DMEM, 2% FCS.

For stability experiments, Vero E6 cells were used as described above. The stability was tested until passage 10, starting from passage 2. After each passage, viral RNAs harvested in supernatants at day 4 were quantified by RT-qPCR. VeroE6 cells were then infected with the supernatant using ten copies of genome per cell. The viruses harvested in supernatants at passages 2, 5, and 10 were sequenced on MiniSeq (Illumina) and analyzed using the public platform Galaxy[48]. Briefly, RNA was extracted from 1ml of supernatant with the QIAamp Viral RNA Mini Kit (Qiagen) according to manufacturer's instructions. The RNAs were rigorously treated with Turbo DNase (Ambion, Thermofisher) and concentrated by ethanol precipitation. Then, cytoplasmic and mitochondrial ribosomal RNAs were removed using the NEBNext® rRNA depletion kit v2 (human/mouse/rat). The libraries were prepared using the NEBNext® ultra II RNA library prep for illumina® with 6 minutes of RNA fragmentation and 16 cycles of amplification. Finally,

quality and the concentration of libraries were determined by using the High Sensitivity D5000 Screentape assay on a TapeStation (Agilent). Sequencing was performed using an illumina Miniseq platform with 150-base paired ends and single indexing for each library. The loading concentration on the flow cell for the sequencing was 1.45pM from a pool of normalized concentration of 18 libraries. For data analysis, reads were trimmed according to the quality score (99%) and length (reads below 80bp were removed) and illumina adapter were deleted using trimmomatic V0.38. Trimmed fastq files were then mapped onto the genome of rescued viruses using bowtie2 V2.4.5 and PCR duplicates were removed using MarkDuplicates. Finally, consensus sequences were called by using ivar consensus and variants were checked on Integrative Genomics Viewer.

MACV, strain Caravallo, GTOV, strain INH-95551, and JUNV, strain P2045 were produced in VeroE6 cells in DMEM, 2% FCS. The clarified cell supernatants were diluted in PBS for inoculation of the animals with the virus. The same viruses were used for further experiments on biological samples from the experiments.

GPC expression by MOPEVAC viruses

VeroE6 cells were infected at a moi of 0.001 and cellular RNAs were extracted at day 0 and day 3 post-infection. RNAs coding for GPC were quantified by RT-qPCR using EurobioGreen One Step Lo-Rox kit (Eurobio). The primers were designed to match all NWAs (Fwd: GCC TGG WGG TTA TTG TYT and Rev: CTC ARC ATG TCA CAG AAY TC). The GAPDH expression was measured using a RT step with oligo dT primers (Superscript III and Oligo dT from Life Technologies) followed by an amplification step with Taqman Gene Expression Master Mix (Applied Biosystems) and a CM probe / primer mix (Applied Biosystems). The expression of GPC was normalized using GAPDH mRNA expression and the ratio expression at day 3 on expression at day 0 calculated to measure the increase of GPC RNA expression after infection.

Western Blot for GP2 detection

MOPEVAC$_{CHA,\ GTO,\ JUN,\ MAC,\ SAB}$ were ultra-centrifugated for 1h30 at 450.000 x g. The pellet was lysed in Laemmli buffer. The amount of lysis solution corresponding to 10^5 ffu was separated on SDS-Page gel 4-12% and transferred on a nitrocellulose membrane. GP2 proteins were detected by staining with the anti-GP2 antibody (KL-AV-2A1[49]) diluted 1/1.000 and anti-mouse HRP diluted 1/20.000 (Jackson ImmunoResearch). Revelation of staining was performed using Super Signal WestDura Extended Duration substrate (ThermoScientific).

ELISA

Virus-specific IgG detection was performed on plasma samples. To produce antigens, VeroE6 cells were infected with wild type viruses. The supernatants were collected at day 4, and diluted with 25% of PEG solution (Abcam). After an overnight incubation at 4°C, the media was centrifuged and the pellet resuspended in buffer containing 1% Triton X-100 (Sigma). The solution was sonicated and frozen. Antigen-negative supernatants were made with the same protocol using uninfected cells. These antigens were coated diluted 1/500 or 1/1,000 in PBS on polysorp 96-microwell plates. After an overnight incubation at 4°C, the wells were blocked for 1 h with PBS, 2.5% BSA. Plasma samples, diluted from 1/250 to 1/16,000 in PBS with 2.5% BSA and 0.5% Tween 20, were added to the wells and the plates incubated for 1 h at 37°C before a final incubation with anti-monkey HRP 1/5,000 (Sigma). Attachment of the conjugated antibody was revealed using TMB and the reaction stopped with orthophosphoric acid. Between each step, the plates were washed three times with PBS, 0.5% Tween 20. The optical density was finally measured and the value obtained from antigen-negative was subtracted from the value of antigen-positive measurements. A sample with a resulting value ≥ 0.1 was defined to be positive. Antibody titers corresponded to the last dilution that was still positive. Statistical differences between conditions were calculated as indicated in figure legends using SigmaPlot 14.5 software (Systat).

IgG detection on 293T cells

293T cells were transfected in 12-well plates with phCMV plasmids coding for GPC gene or the empty vector using Lipofectamine 2000 (Invitrogen). After 2 days of incubation, transfected cells were harvested and divided into 96-well plates. Cells were incubated with Live Dead fixable viability dye (Life Technologies) and plasma samples diluted 1/20 in PBS, 2.5% FCS and 2mM EDTA for 30 min in ice. After two washes in the same buffer, secondary antibody anti-monkey IgG FITC (Southern Biotech) was added to the cells for 30 min at +4°C. Two final washes were performed before fixation with paraformaldehyde 2% and analysis by flow cytometry (Fortessa 4L, BD). The percentage of cells that have bound anti-GPC antibodies was determined on live cells (Kaluza software for flow cytometry analysis).

Quantitative RNA analysis

RNA was prepared from liquid samples using the QIamp viral RNA mini kit (Qiagen), or from cells or tissues using the RNeasy mini kit (QIagen). Quantitative RT-qPCR was performed using the SensiFAST Probe No-ROX One-Step kit (Bioline) on a LightCycler480 device (Roche). A standard RNA was used for quantification; we were able to detect 4 copies viral RNA/µl. We performed a sensitivity test using a different matrix and obtained a limit of quantification of 6 ffu/ml in plasma and oral/nasal swabs for GTOV and 25 ffu/ml in plasma and 625 ffu/ml in swabs for MACV.

Virus titration

Infectious particles were quantified in samples in which viral RNA was detected. For the organs, 10 mg of material was diluted in 100 µl DMEM, 2% FCS and then dispersed for 10 min at 30 beats per second using metal beads. The solution obtained was centrifuged for 3 min at 500 x g to pellet the debris. The supernatant was used for titration.

Samples were serially diluted in DMEM, 2% FCS, added to VeroE6 cells, and the plates incubated for 1 h at 37°C. Medium supplemented with carboxymethylcellulose was added and the plates incubated for one

week. Cells were then fixed for 20 min with 4% formaldehyde. To determine the number of focus-forming units, plates were permeabilized for 5 min with 0.5 % triton, stained for 1 h with anti-virus antibody, and for an addition hour with HRP-conjugated secondary antibody. The reaction was finally revealed using NBT/BCIP (Thermo Scientific). Focus-forming units were counted. To determine the number of plaque-forming units, cells were colored with crystal violet solution (Sigma-Aldrich) diluted 50% in PBS for 10 min, washed with water, and the plaques counted.

MACV and JUNV were revealed using anti-Z MACV and MOPEVAC was stained using anti-Z MOPV. These antibodies were produced in rabbits (Agrobio). For SABV virus, we used an anti-monkey MACV obtained from the USAMRIID. The secondary antibodies were all coupled with HRP (Sigma). We did not obtain reactive antibodies for GTOV but the virus was lytic, and we used crystal violet to reveal plaques. The threshold of detection was 17 ffu/ml for liquid samples and 0.5 ffu/mg for organs.

Seroneutralization

Seroneutralization experiments were conducted using wild type or MOPEVAC viruses, as described in the figure legends. Plasma samples were serially diluted in cell culture medium and a single viral dilution was added to the wells of a 96-well microplate. After a 1 h incubation (37°C/5% CO_2) the plasma/virus mixture was added to cells. The infection was allowed to proceed for 1h and media supplemented with carboxymethylcellulose was added. The cells were incubated for one week before immunostaining of infected cells or crystal violet coloration (cf virus titration). The neutralizing titer was the last dilution that allowed more than a 50% reduction in the number of viral plaques relative to the control condition.

Hematological and biochemical analyses

Hematological parameters were analyzed using a MS9-5s (Melet Schloesing Laboratories) and biochemical analyses were performed on plasma from heparin lithium blood tubes using a Pentra C200 analyzer (Horiba).

Intracellular cytokine staining in PBMCs

Fresh whole blood or PBMCs were stimulated with overlapping peptides of the NP and GPC proteins and stained for flow cytometry analysis, as previously described[26]. Staphylococcal Enterotoxin A (SEA) was used as a positive control. The gating strategy is presented in Extended data 8.

Transcriptomic analyses

Total RNA from PBMCs was extracted using the RNeasy Mini kit (Qiagen) with an on-column DNase step. RNA samples were then quantified using the QuantifluorRNA system (Promega) and qualified using a Standard Sensitivity kit on an Advanced Analytical (AITI fragment analyzer. The External RNA Controls Consortium (ERCC) RNA Spike-in Mix 1 (Thermo Fisher Scientific) was added to all samples to limit sample variability in multiple batches and mRNA was poly(A)-captured using NEXTflex Poly(A) beads (Perkin Elmer). The libraries were prepared using the NEXTflex Rapid Directional RNA-seq (RNA sequencing) Kit (Perkin Elmer), were quantified and qualified using a Quantus quantification kit (Promega) and a fragment analyzer. Sequencing was performed on a NextSeq 500 Flow Cell High OutputSR75 instrument (Illumina) with six samples per flow cell.

Bioinformatics analysis was performed using the RNA-seq pipeline from Sequana[50]. Reads were cleaned of adapter sequences and low-quality sequences using cutadapt version 1.11[51]. Only sequences of at least 25 nucleotides in length were considered for further analysis. STAR version 2.5.0a[52], with default parameters, was used for alignment against the reference genome (Macaca Fascicularis 5 from ENSEMBL version 95). Reads were assigned to genes using featureCounts version 1.4.6-p3[53] from the Subreads package (parameters: -t gene -g ID -O -s 2). Data from these transcriptomic analyses are available on Zenodo DOI: 10.5281/zenodo.7229438[54].

Statistical analyses were performed to identify genes for which the expression profiles were significantly different between each pair of biological conditions. Therefore, statistical tests were performed between each time-point compared to their respective baseline (day 0) within each group. For each data set (post-vaccination and post-challenge), genes exhibiting expression lower than one count per million in at least three samples were considered to have a low level of expression and discarded from the analysis. Differential analysis was performed using the DESeq2 R package (v1.24.0)[55]. The model was adjusted for the effect of vaccination status, time-points, and animal identifier. Gene set enrichment analysis was performed for both data sets to identify gene sets and pathways enriched in the various biological conditions using a one-sided Fisher exact test. The overall gene sets over- or under-expression was tested with a 1-way mixed ANOVA on centered and scaled expressions of the gene set, averaged by condition. The fixed part of the model was adjusted on the groups and timepoints, and the random part was adjusted on the gene identifiers. The Tukey's multiple comparison test was used to compare the timepoints to J0 within each group.

Data availability

The datasets from RNA sequencing generated during the current study are not publicly available due to current analyses still ongoing, but are available from the corresponding author on reasonable request.

Dr. Sylvain Baize is the corresponding author for any request or correspondence: sylvain.baize@pasteur.fr

Acknowledgments

We thank S. Godard, B. Labrosse, C. Leculier, S. Mely, E. Moissonnier, S. Mundweiler, D. Pannetier, A. Pocquet, H. Theoule, and D. Thomas (P4 INSERM–Jean Merieux, US003, INSERM) for BSL4 management during these experiments. We are also grateful to G. Fourcaud, B. Lafoux, and K. Noy for their logistical help. We also thank M. Caroll and R. Hewson (PHE, Porton Down, UK), S. Günther (BNI, Germany) and T.G. Ksiazek (CDC, Atlanta, GA) for providing the Machupo, Guanarito, and Junin viruses and T. G. Ksiazek, P. E. Rollin, and P. Jahrling (Special Pathogens Branch, CDC, Atlanta, GA) for the polyclonal anti-MACV antibodies. Antibody KL-AV-2A1 was a kind gift of F. Krammer (department of Microbiology, Icahn School of Medicine at Mount Sinai, New York). We thank C. Gerke and M-A Dillies for their support in vaccine development and bioinformatics and the "Grand Projet Fédérateur de Vaccinologie" of the Institut Pasteur that funded this project (grant obtained by SB).

Data availability

Data are available in public, open access repositories. For transcriptomic analyses, they are available on Zenodo DOI: 10.5281/zenodo.7229438.

Author contributions

SR managed and performed the experiments, analyzed the results, and wrote the publication. XC performed the reverse genetics experiments to rescue the vaccine candidates. XC, CP, VBC, AJ, MMa, CG, JH, and SB performed the experiments on samples during the animal experiments. LF and PHM were in charge of the animal experiments in the BSL2. CP, VBC, and LA were responsible for the neutralization assays, AJ performed the ELISA experiments and MMa realized the viral titrations in organs. EP and NP computed all transcriptomic data and performed the related analyses. AV, SBar, AD, OL, OJ, and MMo managed animals in the BSL4 facility. MDi was the referent veterinary of this study. MDa and CLL

performed the sequencing for the transcriptomic analyses. HR and CC managed the BSL4 team. SB supervised the entire project.

Competing interests

The authors declare that they have no competing interests. The MOPEVAC vaccine platform described in this study is protected by the U.S. patent 62/245,631, authors listed as co-inventors are SR, SB, XC, MMa, and AJ.

Figure legends

Fig. 1. CM immunization with MOPEVAC$_{MACV}$ induces antibody responses. a. Schematic view of the experiment. The long vertical bars represent each week. The days of vaccination, sampling, challenge, and necropsy are indicated with colored arrows. **b**. Bi-segmented organization of the MOPEVAC$_{MACV}$ genome. The S segment is mutated in the exonuclease domain of the nucleoprotein (NP) and the glycoprotein precursor (GPC) of MACV replaces the GPC of the Mopeia virus (MOPV). The L segment is that of wildtype MOPV (L: polymerase, Z: zinc finger matrix protein, UTR: untranslated regions). **c**. Vero E6 cells were infected at moi = 0.0001 and cell supernatants were collected every day until day 7 and titrated (left graph). Viral titers of the different MOPEVAC at each passage from passage two to ten (right graph). The mean of two experiments is represented for both graphs. **d**. Antibody response during the immunization period. The IgG titer is the last dilution of the plasma sample that is still positive for MACV-specific IgG. Each dot represents an individual value (n = 4). When all samples were negative, dots were not separated. Two-sided Mann-Whitney statistical test was performed to compare IgG values after boost versus after prime at the same day after injection. P values obtained are indicated by an asterisk (*: < 0,05). The neutralization titer corresponds to the last dilution of plasma that still neutralizes more than 50% of wild type MACV. Each curve represents an individual value. The arrow indicates the second vaccine injection.

Fig. 2. Post challenge monitoring of animals and antibody response. a. Clinical score and percentage of the initial body weight at each sampling. **b**. Biochemical parameters measured in plasma samples (ALT/AST: alanine/aspartate aminotransferase). The point represented at day 0 was actually day -9 (reception of the animals). **c**. Viral RNA quantified by RT-qPCR and virus titration performed on positive samples. Negative values are represented at the detection limit. **d**. IgG and neutralization titers are represented as in fig. 1c. One-way Anova test was performed from day 0 to day 12. Significant p values

were obtained only for prime boost group *versus* controls. From day 15, two-sided Mann-Whitney test was performed. Asterisks indicate the p-values (*: <0,05, **<0,01). The optical density obtained by ELISA is represented (at dilution 1/1,000 and 1/250 for prime boost and prime only groups respectively). **e**. Cross-neutralization was evaluated on samples after immunization using MOPEVAC viruses. The arrow indicates the boost.

Fig. 3. Immune responses induced by MOPEVAC$_{NEW}$ in CMs. a. Schematic representation of the protocol. Monkeys were vaccinated or not using a prime-boost strategy (n = 6) and then infected with either MACV or GTOV (four groups, n = 3). The representation is as in fig. 1a. **b**. NAbs were measured during the immunization period and quantified for each pathogenic NWA. The representation is as in fig. 2e. All vaccinated or control animals received the same injections; they are distinguished depending on the future challenge they will receive. **c**. IgG against MACV and GTOV were quantified by ELISA in plasma samples throughout the immunization period. Two-sided Mann-Whitney statistical tests were performed but did not provide significant p-values (n=3). The arrow indicates the second injection of the vaccine. The animals are represented with colors like in b. IgG were also tested on 293T cells expressing GPC from NWAs, MOPV and control cells without GPC expression. The percentage of cells that were recognized by IgG from plasma samples at day 82 post-immunization is represented for each animal.

Fig. 4. Challenge of vaccinated or unvaccinated CMs with GTOV and MACV. Unvaccinated CMs were challenged with GTOV (gray, n = 3) or MACV (red, n = 3). Vaccinated CMs received the same challenge with GTOV (orange, n = 3) or MACV (blue, n = 3) **a**. The clinical score and weight loss were evaluated at each sampling as in fig. 2a. **b**. Viral RNA was quantified by RT-qPCR at each sampling. We performed the quantification of infectious viruses on RT-qPCR positive samples. Negative values are represented at the threshold of detection.

Fig. 5. Antibody response after challenge. The colors used are the same as in Fig. 4. **a**. IgG titers were evaluated by ELISA and represent the last dilution of plasma that is still positive. The dots indicate individual values. Two-sided Mann-Whitney statistical tests were performed but did not provide significant p-values. **b**. Neutralization titers were defined against wildtype viruses at days 0, 12, and the date of necropsy. The experiment was performed as for fig. 1c. **c**. MOPEVAC viruses were used to evaluate the neutralization titers. The experiment was performed using the same protocol.

Fig. 6. Immune responses after immunization and challenge. a. Transcriptomic analysis of PBMCs after immunization. The heatmaps represent the genes expressions in each pathway. The color of the heatmaps represents the mean of scaled normalized counts for each group and time-point (Vacc: n=4, Ctrl n=3). Box plots show the average of the normalized gene expression of the pathway (central line: median; hinges: first and third quartiles; whiskers: largest or smallest value no further than 1.5 inter-quartile range from the hinge). Outlying points are plotted individually. Significant differences were tested using 1-way mixed ANOVA on centered and scaled expressions of the gene set, averaged by condition. The Tukey's multiple comparison test was used to compare the timepoints to J0 within each group. Asterisks indicate the difference from day 0 (***$p < 0.001$, **$p < 0.01$, *$p < 0.05$) and exact p values are provided (Supp. Table 3). **b**. Transcriptomic analysis of PBMCs after challenge. Data were analyzed and represented as in a (n=3).

References

1. Charrel, R. N., de Lamballerie, X. & Fulhorst, C. F. The Whitewater Arroyo virus: natural evidence for genetic recombination among Tacaribe serocomplex viruses (family Arenaviridae). *Virology* **283**, 161–166 (2001).

2. Choe, H., Jemielity, S., Abraham, J., Radoshitzky, S. R. & Farzan, M. Transferrin receptor 1 in the zoonosis and pathogenesis of New World hemorrhagic fever arenaviruses. *Curr. Opin. Microbiol.* **14**, 476–482 (2011).

3. Ambrosio, A., Saavedra, M., Mariani, M., Gamboa, G. & Maiza, A. Argentine hemorrhagic fever vaccines. *Hum. Vaccin.* **7**, 694–700 (2011).

4. Enria, D. A., Briggiler, A. M. & Sánchez, Z. Treatment of Argentine hemorrhagic fever. *Antiviral Res.* **78**, 132–139 (2008).

5. Enria, D. A. *et al.* [Candid#1 vaccine against Argentine hemorrhagic fever produced in Argentina. Immunogenicity and safety]. *Medicina (B. Aires).* **70**, 215–22 (2010).

6. Albariño, C. G. *et al.* The major determinant of attenuation in mice of the Candid1 vaccine for Argentine hemorrhagic fever is located in the G2 glycoprotein transmembrane domain. *J. Virol.* **85**, 10404–8 (2011).

7. York, J. & Nunberg, J. H. Epistastic Interactions within the Junín Virus Envelope Glycoprotein Complex Provide an Evolutionary Barrier to Reversion in the Live-Attenuated Candid#1 Vaccine. *J. Virol.* **92**, (2018).

8. Aguilar, P. V *et al.* Reemergence of Bolivian hemorrhagic fever, 2007-2008. *Emerg. Infect. Dis.* **15**,

1526–1528 (2009).

9. Patterson, M., Grant, A. & Paessler, S. Epidemiology and pathogenesis of Bolivian hemorrhagic fever. *Curr. Opin. Virol.* **5**, 82–90 (2014).

10. Johnson, D. M. *et al.* Bivalent Junin & Machupo experimental vaccine based on alphavirus RNA replicon vector. *Vaccine* **38**, 2949–2959 (2020).

11. Koma, T. *et al.* Machupo Virus Expressing GPC of the Candid#1 Vaccine Strain of Junin Virus Is Highly Attenuated and Immunogenic. *J. Virol.* **90**, 1290–1297 (2016).

12. Coimbra, T. L. . *et al.* New arenavirus isolated in Brazil. *Lancet* **343**, 391–392 (1994).

13. Tesh, R. B., Jahrling, P. B., Salas, R. & Shope, R. E. Description of Guanarito virus (Arenaviridae: Arenavirus), the etiologic agent of Venezuelan hemorrhagic fever. *Am. J. Trop. Med. Hyg.* **50**, 452–459 (1994).

14. Delgado, S. *et al.* Chapare virus, a newly discovered arenavirus isolated from a fatal hemorrhagic fever case in Bolivia. *PLoS Pathog.* **4**, e1000047 (2008).

15. Ellis, B. A. *et al.* A Longitudinal Study of Junin Virus Activity in the Rodent Reservoir of Agrentine Hemorrhagic Fever. *Am. J. Trop. Med. Hyg.* **47**, 749–763 (1992).

16. Mills, J. N. *et al.* Junin virus activity in rodents from endemic and nonendemic loci in central Argentina. *Am. J. Trop. Med. Hyg.* **44**, 589–597 (1991).

17. Mercado, R. Rodent control programmes in areas affected by Bolivian haemorrhagic fever. *Bull. World Health Organ.* **52**, 691–6 (1975).

18. Fulhorst, C. F. *et al.* Isolation and characterization of Whitewater Arroyo virus, a novel North American arenavirus. *Virology* **224**, 114–120 (1996).

19. Fatal illnesses associated with a new world arenavirus--California, 1999-2000. *MMWR. Morb. Mortal. Wkly. Rep.* **49**, 709–711 (2000).

20. Briese, T. *et al.* Genetic Detection and Characterization of Lujo Virus, a New Hemorrhagic Fever–Associated Arenavirus from Southern Africa. *PLoS Pathog.* **5**, e1000455 (2009).

21. Enria, D. A., Briggiler, A. M., Fernandez, N. J., Levis, S. C. & Maiztegui, J. I. Importance of dose of neutralising antibodies in treatment of Argentine haemorrhagic fever with immune plasma. *Lancet (London, England)* **2**, 255–256 (1984).

22. Kenyon, R. H., Green, D. E., Eddy, G. A. & Peters, C. J. Treatment of Junin Virus-Infected Guinea Pigs With Immune Serum: Development of Late Neurological Disease. *J. Med. Virol.* **20**, 207–218 (1986).

23. Avila, M. M., Samoilovich, S. R., Laguens, R. P., Merani, M. S. & Weissenbacher, M. C. Protection of Junín virus-infected marmosets by passive administration of immune serum: association with late neurologic signs. *J. Med. Virol.* **21**, 67–74 (1987).

24. Maiztegui, J. I., Fernandez, N. J. & de Damilano, A. J. Efficacy of immune plasma in treatment of Argentine haemorrhagic fever and association between treatment and a late neurological syndrome. *Lancet (London, England)* **2**, 1216–1217 (1979).

25. Carnec, X. *et al.* A Vaccine Platform against Arenaviruses Based on a Recombinant Hyperattenuated Mopeia Virus Expressing Heterologous Glycoproteins. *J. Virol.* **92**, (2018).

26. Mateo, M. *et al.* Vaccines inducing immunity to Lassa virus glycoprotein and nucleoprotein protect macaques after a single shot. *Sci. Transl. Med.* **11**, (2019).

27. Luis, M.-S. *et al.* Identification of Amino Acid Residues Critical for the Anti-Interferon Activity of the Nucleoprotein of the Prototypic Arenavirus Lymphocytic Choriomeningitis Virus. *J. Virol.* **83**,

11330–11340 (2009).

28. Jiang, X. *et al.* Structures of arenaviral nucleoproteins with triphosphate dsRNA reveal a unique mechanism of immune suppression. *J. Biol. Chem.* **288**, 16949–16959 (2013).

29. Habjan, M. *et al.* Processing of genome 5' termini as a strategy of negative-strand RNA viruses to avoid RIG-I-dependent interferon induction. *PLoS One* **3**, e2032 (2008).

30. Hastie, K. M., Kimberlin, C. R., Zandonatti, M. A., MacRae, I. J. & Saphire, E. O. Structure of the Lassa virus nucleoprotein reveals a dsRNA-specific 3' to 5' exonuclease activity essential for immune suppression. *Proc. Natl. Acad. Sci. U. S. A.* **108**, 2396–2401 (2011).

31. Nakaya, H. I. *et al.* Systems Analysis of Immunity to Influenza Vaccination across Multiple Years and in Diverse Populations Reveals Shared Molecular Signatures. *Immunity* **43**, 1186–1198 (2015).

32. Frank, M. G. *et al.* South American Hemorrhagic Fevers: A summary for clinicians. *Int. J. Infect. Dis.* **105**, 505–515 (2021).

33. Golden, J. W. *et al.* An attenuated Machupo virus with a disrupted L-segment intergenic region protects guinea pigs against lethal Guanarito virus infection. *Sci. Rep.* **7**, 4679 (2017).

34. Leske, A. *et al.* Assessing cross-reactivity of Junín virus-directed neutralizing antibodies. *Antiviral Res.* **163**, 106–116 (2019).

35. Silva-Ramos, C. R., Faccini-Martínez, Á. A., Calixto, O.-J. & Hidalgo, M. Bolivian hemorrhagic fever: A narrative review. *Travel Med. Infect. Dis.* **40**, 102001 (2021).

36. Escalera-Antezana, J. P. *et al.* Clinical features of fatal cases of Chapare virus hemorrhagic fever originating from rural La Paz, Bolivia, 2019: A cluster analysis. *Travel Med. Infect. Dis.* **36**, 101589 (2020).

686 37. Rodríguez-Morales, A. J., Bonilla-Aldana, D. K., Risquez, A., Paniz-Mondolfi, A. & Suárez, J. A.
687 Should we be concerned about Venezuelan hemorrhagic fever? - A reflection on its current
688 situation in Venezuela and potential impact in Latin America amid the migration crisis. *New*
689 *microbes new Infect.* **44**, 100945 (2021).

690 38. Ellwanger, J. H. & Chies, J. A. B. Keeping track of hidden dangers - The short history of the Sabiá
691 virus. *Rev. Soc. Bras. Med. Trop.* **50**, 3–8 (2017).

692 39. Medaglini, D., Harandi, A. M., Ottenhoff, T. H. M., Siegrist, C.-A. & Consortium, V.-E. Ebola vaccine
693 R&D: Filling the knowledge gaps. *Sci. Transl. Med.* **7**, 317ps24-317ps24 (2015).

694 40. M., N. W. *et al.* Contrasting Modes of New World Arenavirus Neutralization by Immunization-
695 Elicited Monoclonal Antibodies. *MBio* **0**, e02650-21 (2022).

696 41. Clark, L. E. *et al.* Vaccine-elicited receptor-binding site antibodies neutralize two New World
697 hemorrhagic fever arenaviruses. *Nat. Commun.* **9**, 1884 (2018).

698 42. Sommerstein, R. *et al.* Arenavirus Glycan Shield Promotes Neutralizing Antibody Evasion and
699 Protracted Infection. *PLOS Pathog.* **11**, e1005276 (2015).

700 43. Bonhomme, C. J. *et al.* Glycosylation modulates arenavirus glycoprotein expression and function.
701 *Virology* **409**, 223–233 (2011).

702 44. Huang, C. *et al.* Highly Pathogenic New World and Old World Human Arenaviruses Induce Distinct
703 Interferon Responses in Human Cells. *J. Virol.* **89**, 7079–7088 (2015).

704 45. Levis, S. C. *et al.* Correlation between endogenous interferon and the clinical evolution of patients
705 with Argentine hemorrhagic fever. *J. Interferon Res.* **5**, 383–389 (1985).

706 46. Marta, R. F. *et al.* Proinflammatory cytokines and elastase-alpha-1-antitrypsin in Argentine
707 hemorrhagic fever. *Am. J. Trop. Med. Hyg.* **60**, 85–89 (1999).

47. Mateer, E. J., Maruyama, J., Card, G. E., Paessler, S. & Huang, C. Lassa Virus, but Not Highly Pathogenic New World Arenaviruses, Restricts Immunostimulatory Double-Stranded RNA Accumulation during Infection. *J. Virol.* **94**, e02006-19 (2020).

48. Afgan, E. *et al.* The Galaxy platform for accessible, reproducible and collaborative biomedical analyses: 2018 update. *Nucleic Acids Res.* **46**, W537–W544 (2018).

49. Amanat, F. *et al.* Antibodies to the Glycoprotein GP2 Subunit Cross-React between Old and New World Arenaviruses. *mSphere* **3**, e00189-18 (2018).

50. Cokelaer, T., Desvillechabrol, D., Legendre, R. & Cardon, M. 'Sequana': a Set of Snakemake NGS pipelines. *J. Open Source Softw.* **2**, 352 (2017).

51. Martin, M. Cutadapt removes adapter sequences from high-throughput sequencing reads. *EMBnet.journal; Vol 17, No 1 Next Gener. Seq. Data Anal. - 10.14806/ej.17.1.200* (2011).

52. Dobin, A. *et al.* STAR: ultrafast universal RNA-seq aligner. *Bioinformatics* **29**, 15–21 (2013).

53. Liao, Y., Smyth, G. K. & Shi, W. featureCounts: an efficient general purpose program for assigning sequence reads to genomic features. *Bioinformatics* **30**, 923–930 (2014).

54. Baize, S. The MOPEVAC multivalent vaccine induces sterile protection against New World Arenaviruses in non-human primates. (2022) doi:10.5281/ZENODO.7229439.

55. Love, M. I., Huber, W. & Anders, S. Moderated estimation of fold change and dispersion for RNA-seq data with DESeq2. *Genome Biol.* **15**, 550 (2014).

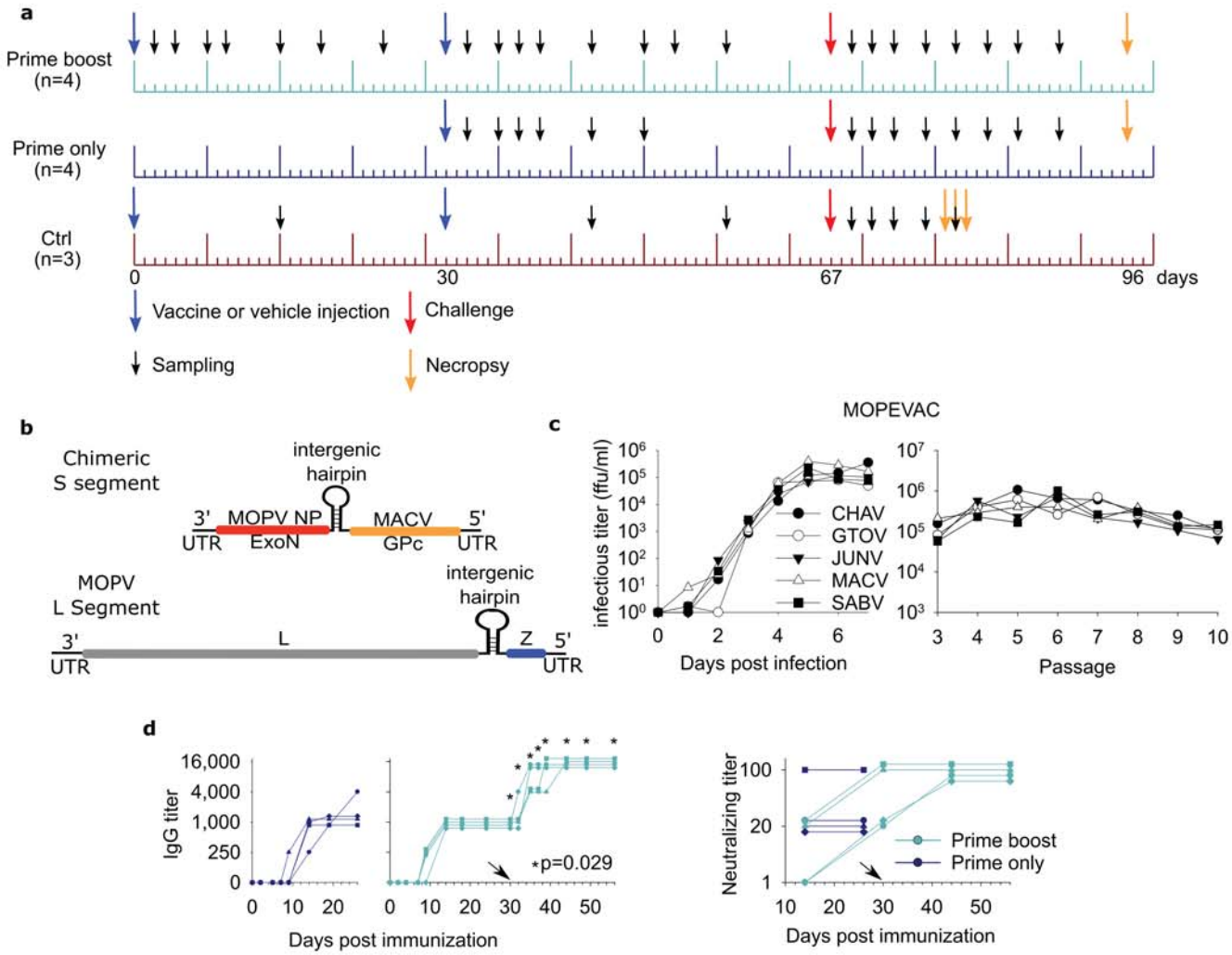

Fig. 1: CM immunization with MOPEVACMACV induces Ab responses.

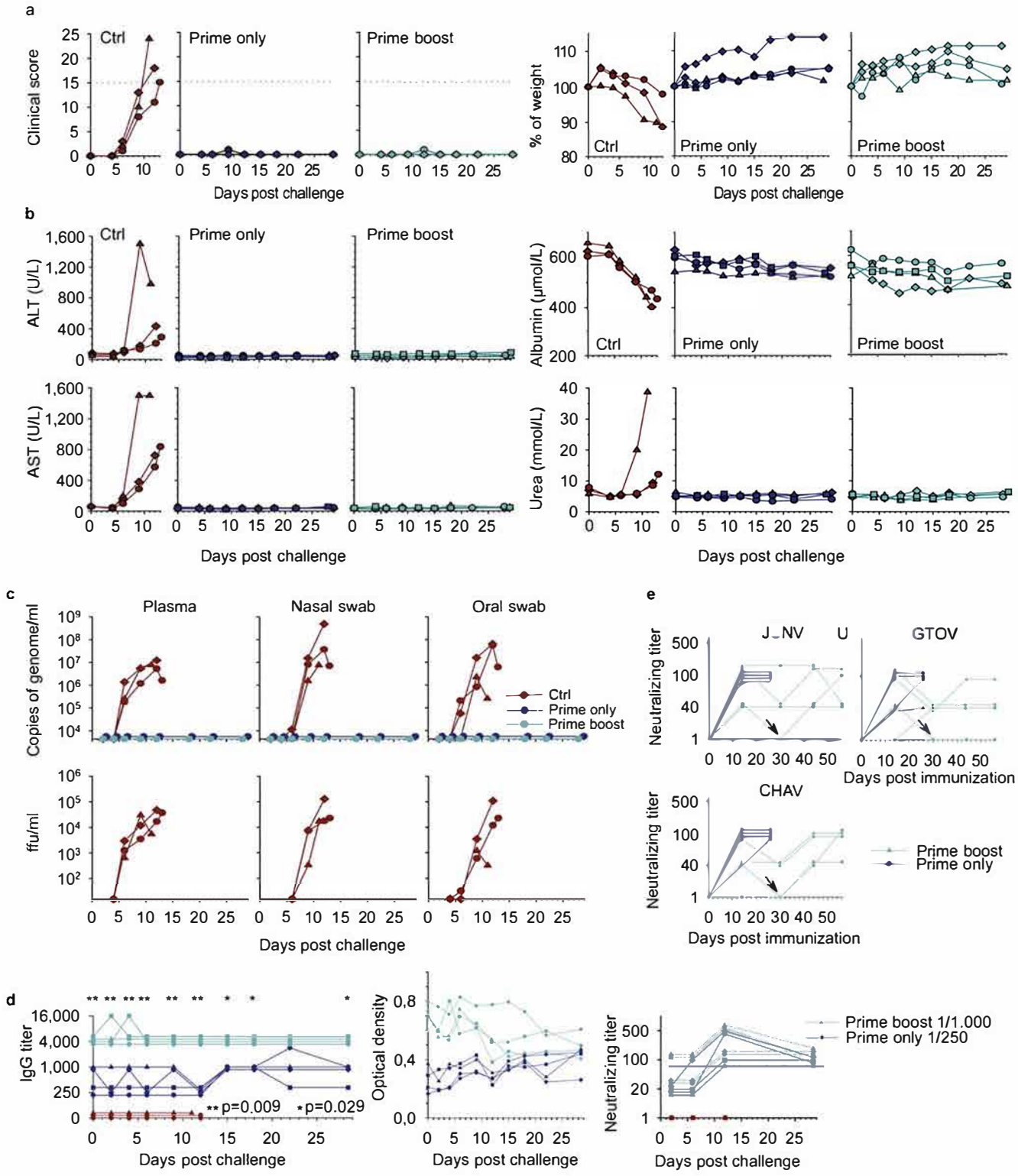

Fig. 2. Post challenge monitoring of animals and antibody response

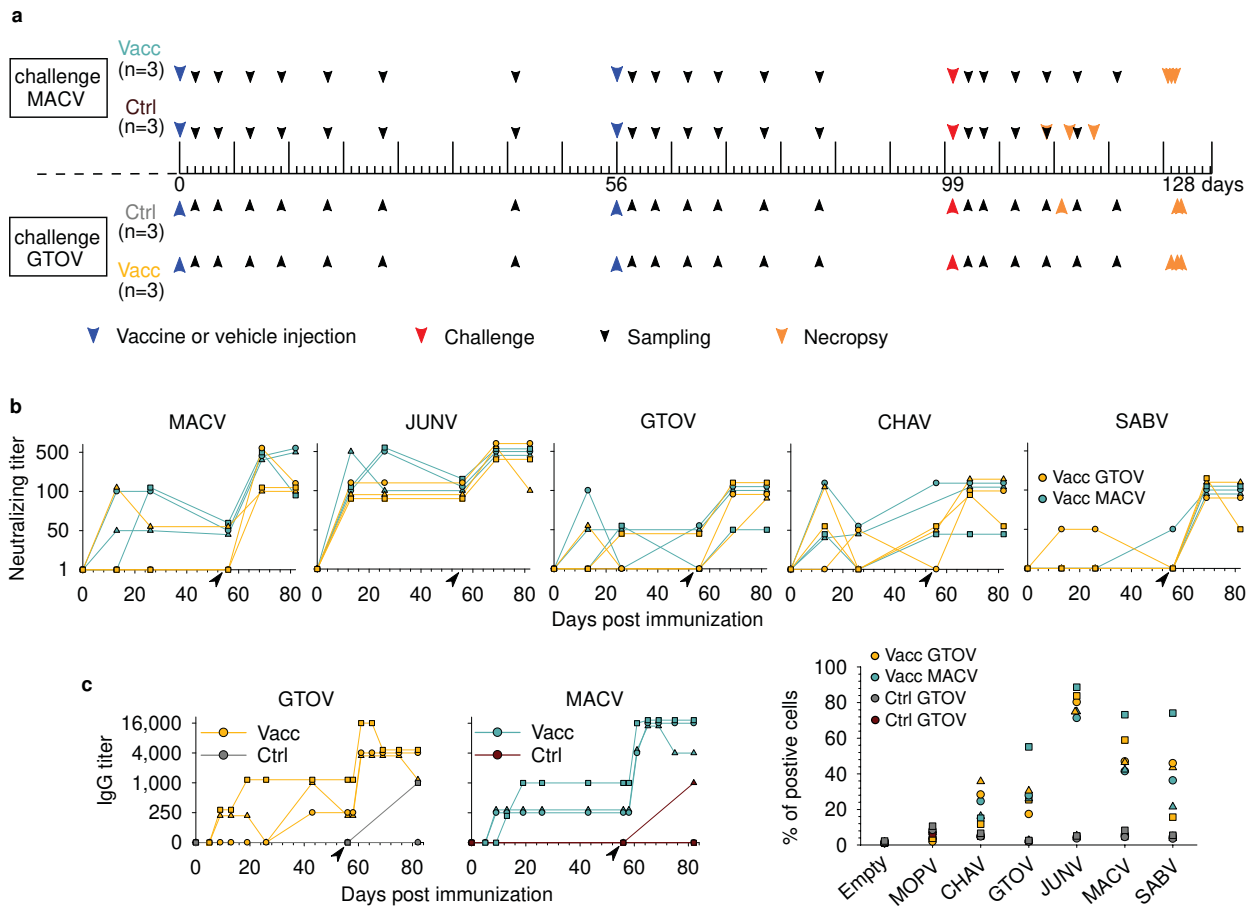

Fig. 3: Immune responses induced by MOPEVACNEW in CMs

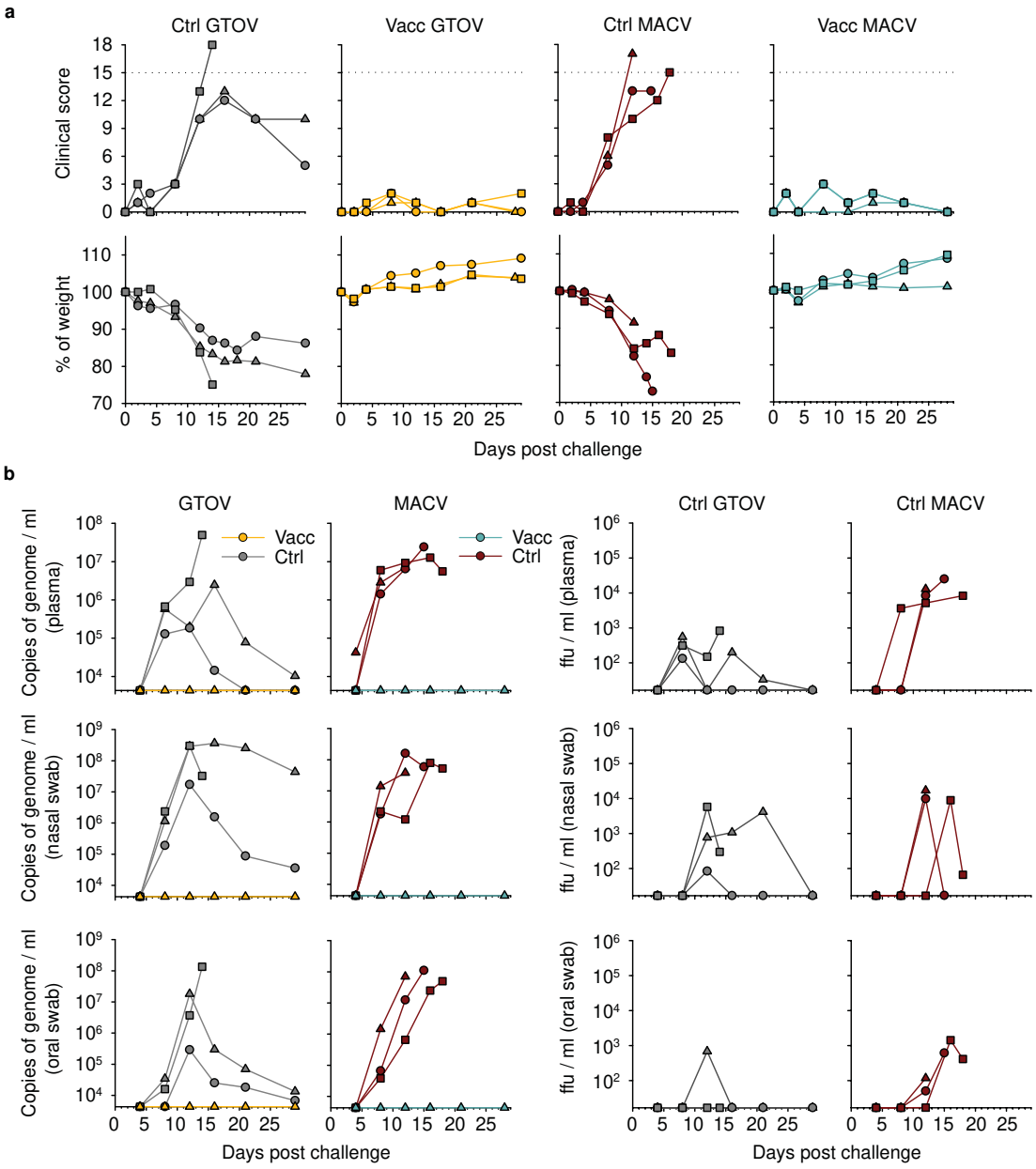

Fig. 4. Challenge of vaccinated or unvaccinated CMs with GTOV and MACV

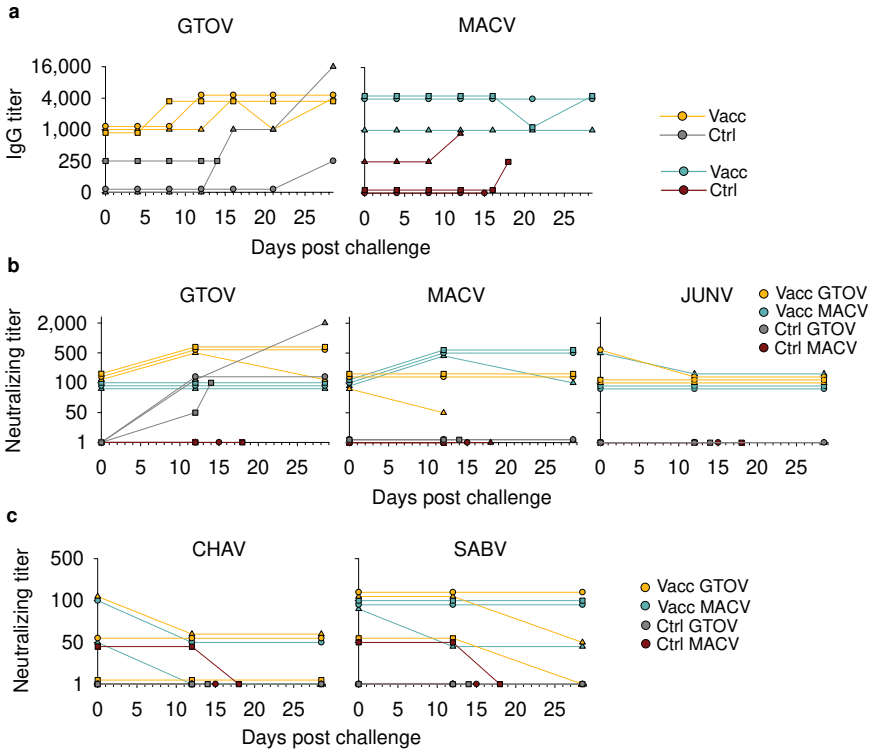

Fig. 5. Antibody response after challenge

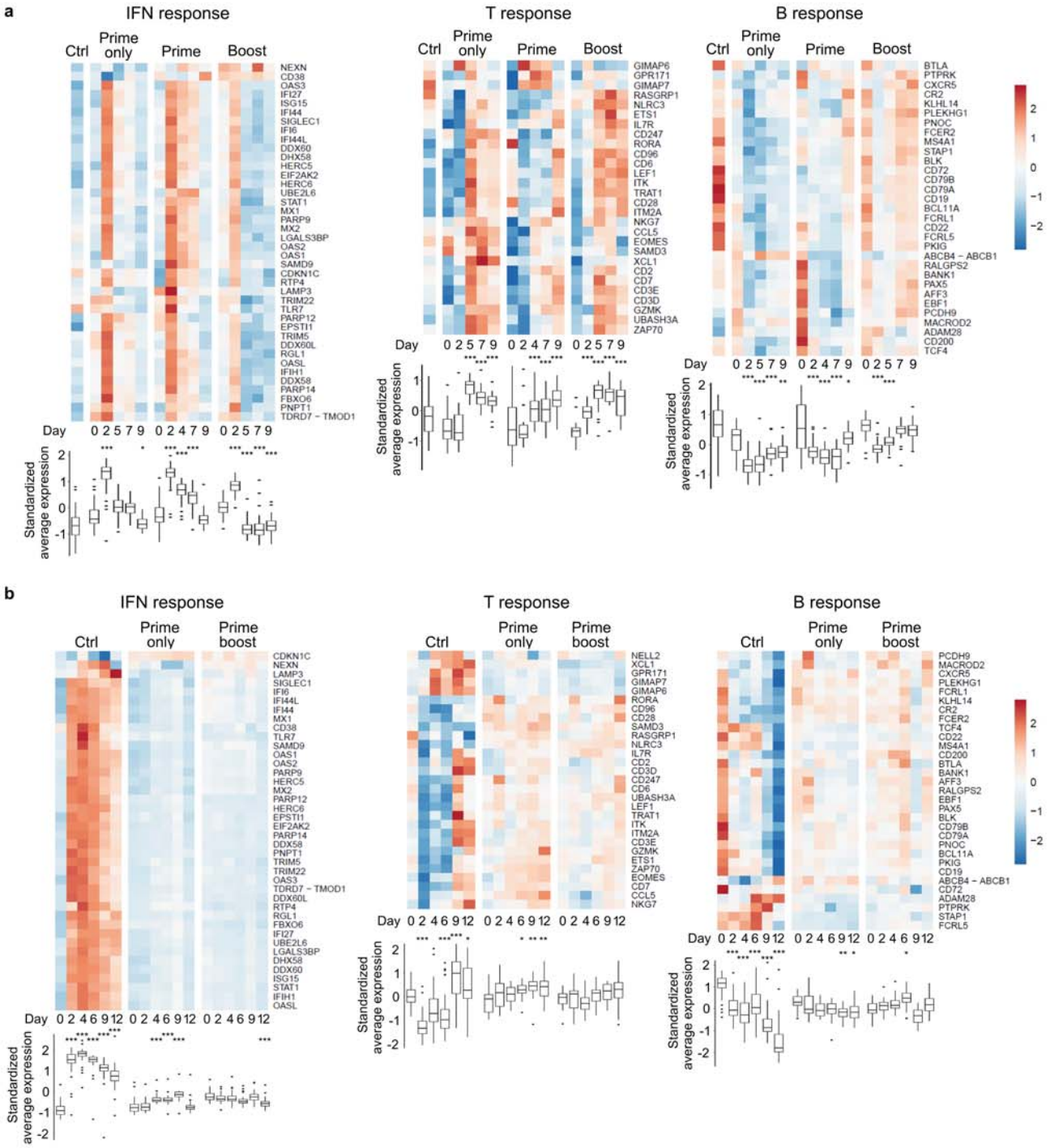

Fig. 6. Immune responses after immunization and challenge

Figure #	Figure title One sentence only	Filename This should be the name the file is saved as when it is uploaded to our system. Please include the file extension. i.e.: *Smith_ED_Fig1.jpg*	Figure Legend If you are citing a reference for the first time in these legends, please include all new references in the main text Methods References section, and carry on the numbering from the main References section of the paper. If your paper does not have a Methods section, include all new references at the end of the main Reference list.
Extended Data Fig. 1	**GPs expression by MOPEVAC viruses**	Ext_data_Fig1.pdf	**a.** VeroE6 cells were infected at a moi of 0.001 and cellular RNAs were extracted at day 0 and day 3 post-infection. The ratio of GPC expression of day 3 relative to day 0 was calculated and represented for each MOPEVAC virus. **b.** Expression of GP2 detected by KL-AV-2A1[49] antibody. GP2 protein expression was detected by western blot from 10^5 ffu of MOPEVAC viruses, in a single experiment. The antibody has been described to detect JUNV, GTOV and MACV but its binding on CHAV and SABV was not known. These results show the expression by the different MOPEVAC viruses of the GP2 proteins of all NWA except the one of SABV, probably because of a lack of cross-reactivity of the antibody.
Extended Data Fig. 2	**Real-time recording of body temperature after challenge**	Ext_data_Fig2.pdf	Recording systems were implanted in the CMs to evaluate the body temperature throughout the protocol. A number were defective. We thus obtained data for seven CMs: the three controls, three prime only vaccinated animals, and one prime boost. The recording was stopped unintentionally for a small period for five animals, this is clearly visible in the graphs.
Extended Data Fig. 3	**Hematological parameters and viral loads in the organs at the day of necropsy**	Ext_data_Fig3.pdf	**a**. Cell counts and hemoglobin concentrations in whole blood were measured at each sampling. **b**. Viral RNA was quantified by RT-qPCR from crushed organs or cells. RT-qPCR-positive samples were evaluated for infectious virus titers. Li: liver, mLN: mesenteric lymph node, iLN: inguinal lymph node, Ki:

			kidney, Lu: lung, Bl: bladder, AG: adrenal gland, Br: brain, Ce: cerebellum, Sp: spleen, Spleno: splenocytes.
Extended Data Fig. 4	**Body temperature before and after challenge in the MOPEVAC$_{NEW}$ experiment**	Ext_data_Fig4.pdf	Intraperitoneal implants recorded the body temperature throughout the experiment at 15-min intervals. **a**. Post immunization period in vaccinated CMs. All received the same vaccine, but the color indicates the virus used for the challenge. **b**. Body temperature of vaccinated and control animals after challenge.
Extended Data Fig. 5	**Gating strategy for determination of IgG fixation on GPs**	Ext_data_Fig5.pdf	The gates used to quantify the cells expressing or not GPs that fixed IgG from plasma are presented. FSC / SSC was used to gate cells, then singlets were determined using SSC / SSC-W and live cells were gated: Live Dead negative cells. The cells that fixed IgG and the secondary anti-IgG FITC were defined with the gate "Positive". Three conditions of the same plasma sample are presented for comparison: empty vector, cells expressing GPs of MOPV and cells expressing GPS of JUNV.
Extended Data Fig. 6	**Viral loads in organs and immune-preserved compartments**	Ext_data_Fig6.pdf	**a.** Viral RNA was quantified by RT-qPCR from crushed organs or cells. RT-qPCR-positive samples were evaluated for infectious virus titers. **b.** Viral RNA was quantified from cerebrospinal fluid (CSF) and eye vitreous humor and infectious virus titration was also performed. Li: liver, mLN: mesenteric lymph node, iLN: inguinal lymph node, Ki: kidney, Lu: lung, Bl: bladder, AG: adrenal gland, Br: brain, Ce: cerebellum, LI: large intestine, SI: small intestine, Ov: ovary, Pa: pancreas, Th: thymus, Sp: spleen, Spleno: splenocytes.
Extended Data Fig. 7	**Hematological and biochemical parameters after challenge in the**	Ext_data_Fig7.pdf	**a.** Cell counts and hemoglobin concentrations were measured at each sampling after challenge. **b.** Biochemical parameters were assayed in plasma at each sampling. C-reactive protein (CRP), alanine aminotransferase (ALT), aspartate

	MOPEVAC$_{NEW}$ experiment		aminotransferase (AST), and plasmatic albumin levels are presented.
Extended Data Fig. 8	**Gating strategy for flow cytometry analysis**	Ext_data_Fig8.pdf	The gates used to quantify IFNγ-producing and CD154-expressing T cells are presented for an unstimulated sample (a) and for the same sample stimulated with staphylococcus-enterotoxin A (SEA), as a positive control (b). FSCint/FSCtof was used to select singlets (singlets gate). Then, dead cells are excluded using live-dead staining (live gate). Lymphocytes were selected using FSCint/SSCint parameters (LC gate). Then, CD4+ and CD8+ T cells were selected using CD3/CD4 and CD3/CD8 staining (CD4+ and CD8+ gates). Finally, the percentage of IFNγ-producing and CD154-expressing CD4+ and CD8+ T cells is determined using a quadrant in the IFNγ/CD154 dotplot. c. A similar strategy was applied for CD137 and GrzB detection.
Extended Data Fig. 9	**Activation of T cells in response to peptide stimulation**	Ext_data_Fig9.pdf	**a.** PBMCs sampled at days 14 and 24 post-prime and day 19 post-boost were stimulated with overlapping peptides covering MACV NP and GP and LASV NP. SEA was used as a positive control. After an overnight incubation, the cells were stained with conjugated antibodies and analyzed by flow cytometry for the expression of CD154, CD137, GrzB and IFNγ. Expression values represent the difference between stimulated and non-stimulated cells. Light blue dots represent animals vaccinated with a prime-boost strategy (n=4, except for J19 boost where SEA n=2, NP LASV n=3) and black dots the control animals (n=3). The dots were not separated when the expression values were close to 0. **b.** After challenge, peptide stimulation was performed on whole blood. GPC and NP specific T cell responses were evaluated. The difference from

			the non-stimulated condition is represented (Ctrl: n=3, Vacc: n=4). The SEA control at day 0 is presented for comparison.
Extended Data Fig. 10			

2

Item	Present?	Filename This should be the name the file is saved as when it is uploaded to our system, and should include the file extension. The extension must be .pdf	A brief, numerical description of file contents. i.e.: *Supplementary Figures 1-4, Supplementary Discussion, and Supplementary Tables 1-4.*
Supplementary Information	Choose an item.		
Reporting Summary	Choose an item.		
Peer Review Information	Choose an item.	*OFFICE USE ONLY*	

3

Type	Number If there are multiple files of the same type this should be the numerical indicator. i.e. "1" for Video 1, "2" for Video 2, etc.	Filename This should be the name the file is saved as when it is uploaded to our system, and should include the file extension. i.e.: *Smith_ Supplementary_Video_1.mov*	Legend or Descriptive Caption Describe the contents of the file
Supplementary Table	1	Supp_Tables	**Evolution of vaccine candidate genomes during serial passages in VeroE6 cells.** The consensus genome sequences of the five vaccine candidates were determined at passages 2, 5, and

			10 and compared to the initial sequences (P2). The changes in codon sequences were indicated as well as the position of the mutation in the genome. The amino acid changes are indicated for non synonymous mutations whereas synonymous mutations are colored in green. The passage after which the mutation has been detected is indicated by the presence of a colored box.
Supplementary Table	2	Supp_Tables	Parameters used to establish the clinical score after challenge and their respective values
Supplementary Table	3	Supp_Tables	**Exact p values corresponding to figure 6.** For each condition the comparison was made with the day 0 timepoint.
Choose an item.			
Choose an item.			
Choose an item.			

4

Parent Figure or Table	Filename This should be the name the file is saved as when it is uploaded to our system, and should include the file extension. i.e.:	Data description i.e.: Unprocessed Western Blots and/or gels, Statistical Source Data, etc.

	Smith_SourceData_Fig1.xls, or *Smith_ Unmodified_Gels_Fig1.pdf*	
Source Data Fig. 1		
Source Data Fig. 2		
Source Data Fig. 3		
Source Data Fig. 4		
Source Data Fig. 5		
Source Data Fig. 6		
Source Data Fig. 7		
Source Data Fig. 8		
Source Data Extended Data Fig. 1		
Source Data Extended Data Fig. 2		
Source Data Extended Data Fig. 3		
Source Data Extended Data Fig. 4		
Source Data Extended Data Fig. 5		
Source Data Extended Data Fig. 6		

Source Data Extended Data Fig. 7		
Source Data Extended Data Fig. 8		
Source Data Extended Data Fig. 9		
Source Data Extended Data Fig. 10		

Extended Data Fig. 1

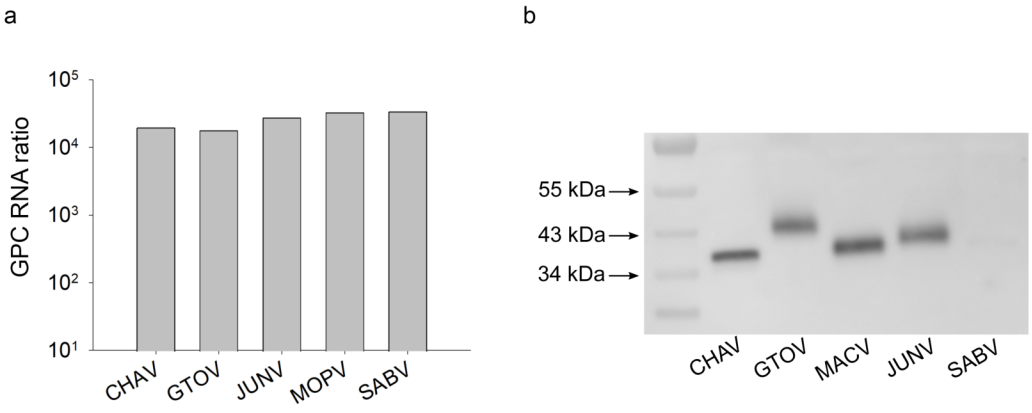

Extended Data Fig. 2

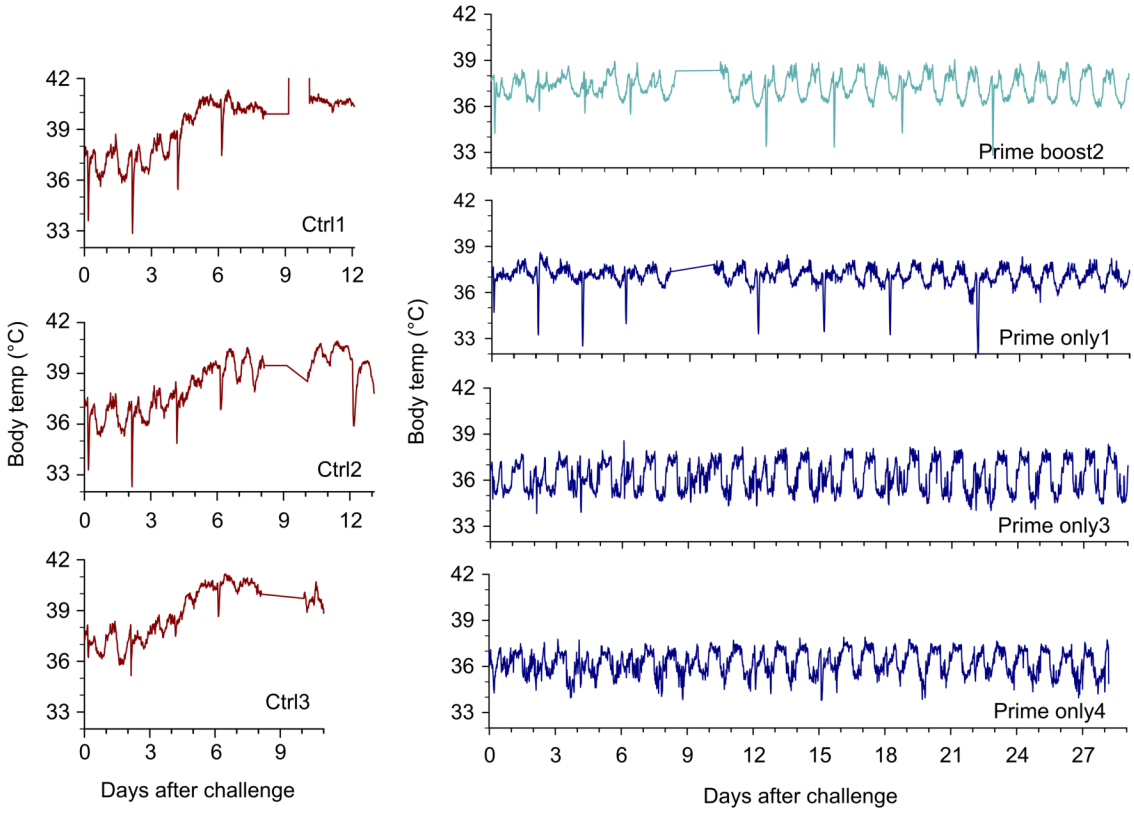

Extended Data Fig. 3

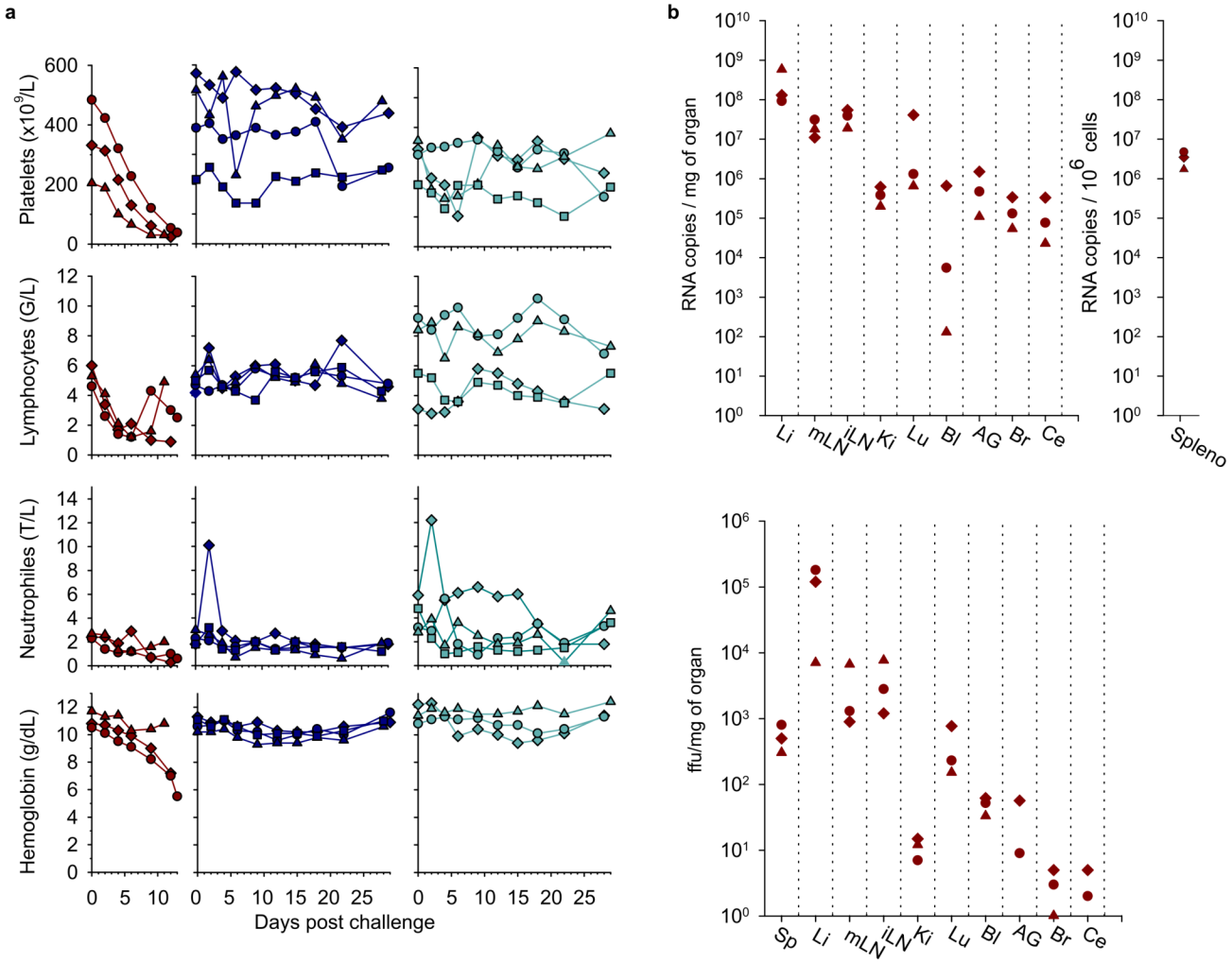

Extended Data Fig. 4

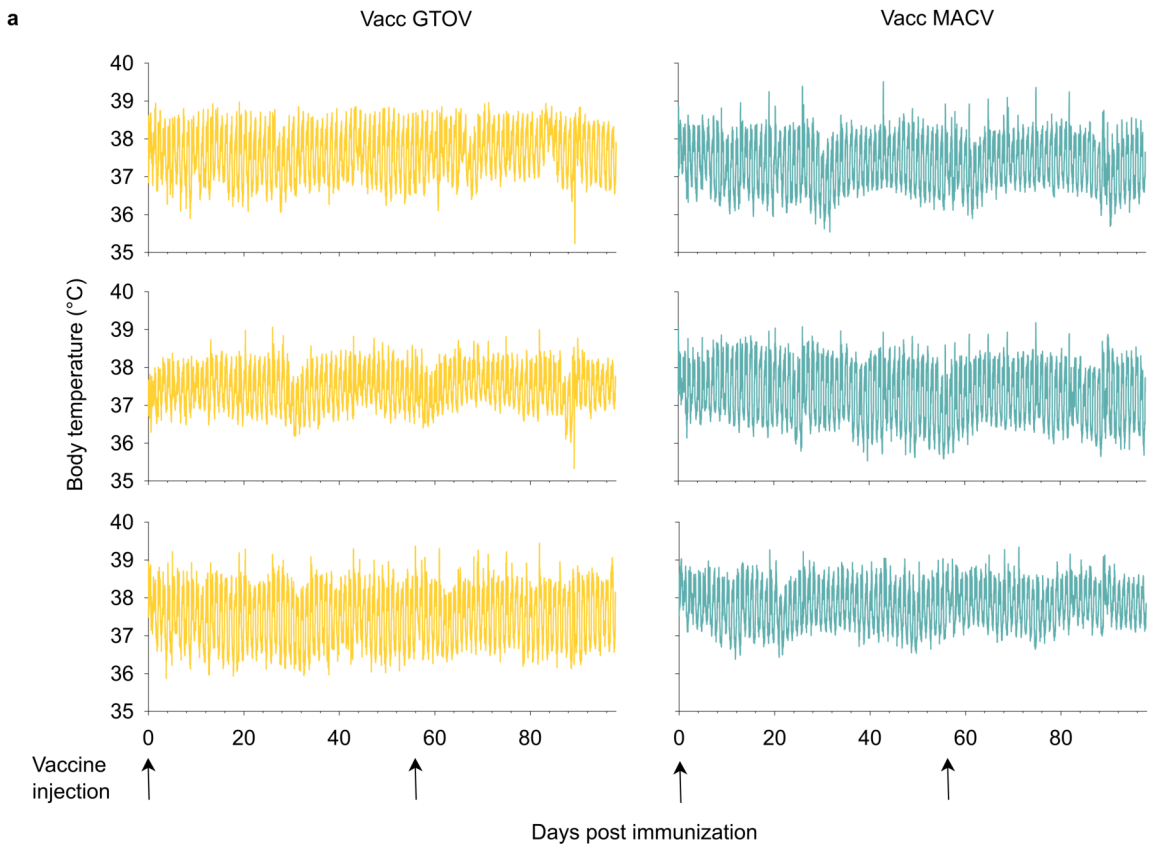

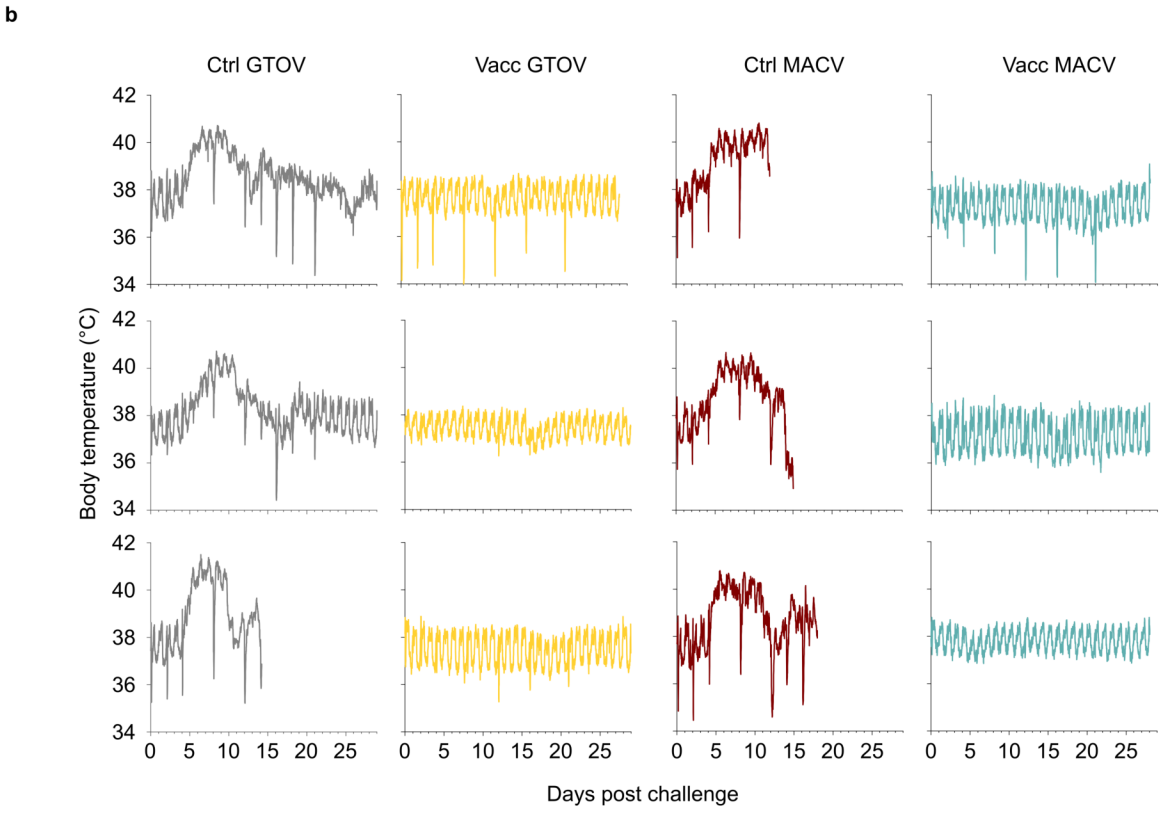

Extended Data Fig. 5

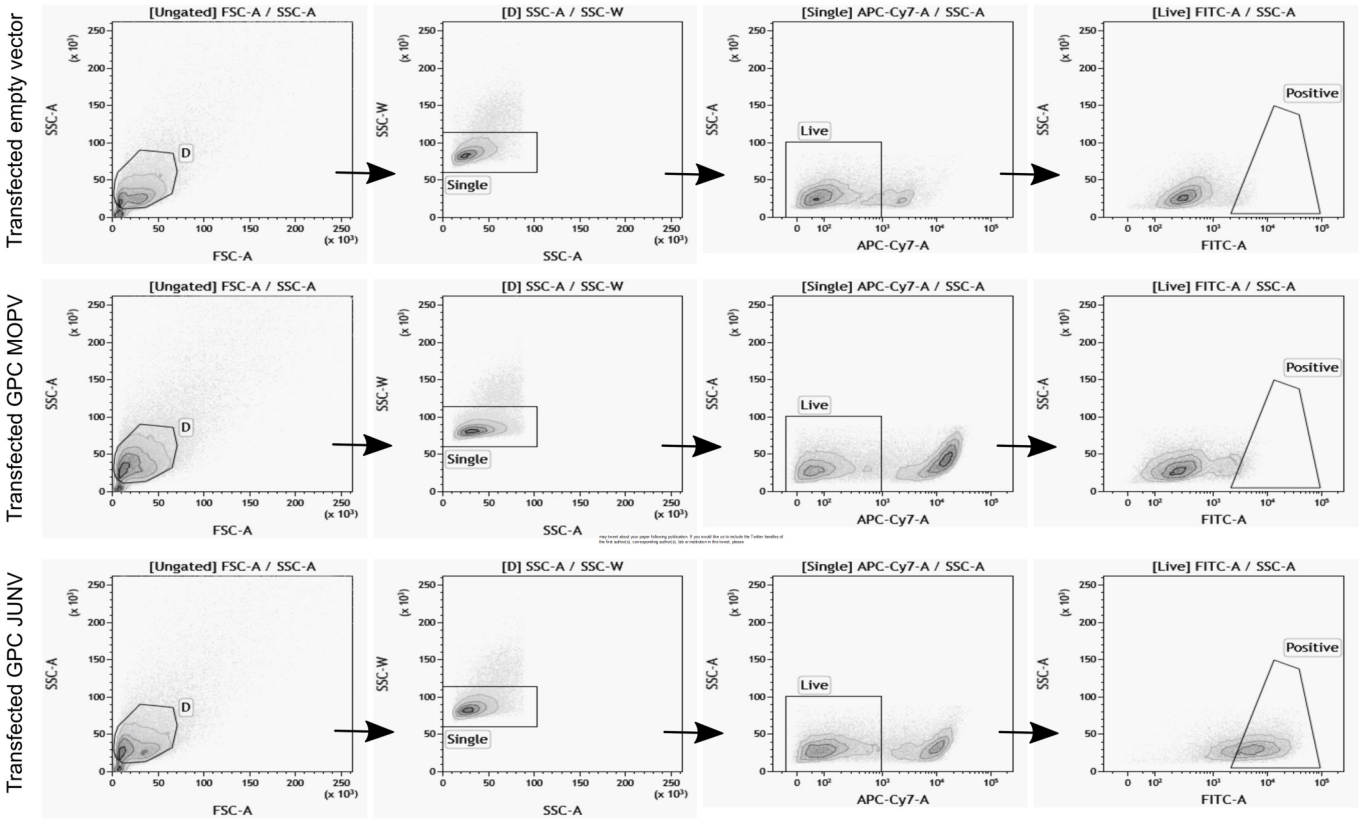

Extended Data Fig. 6

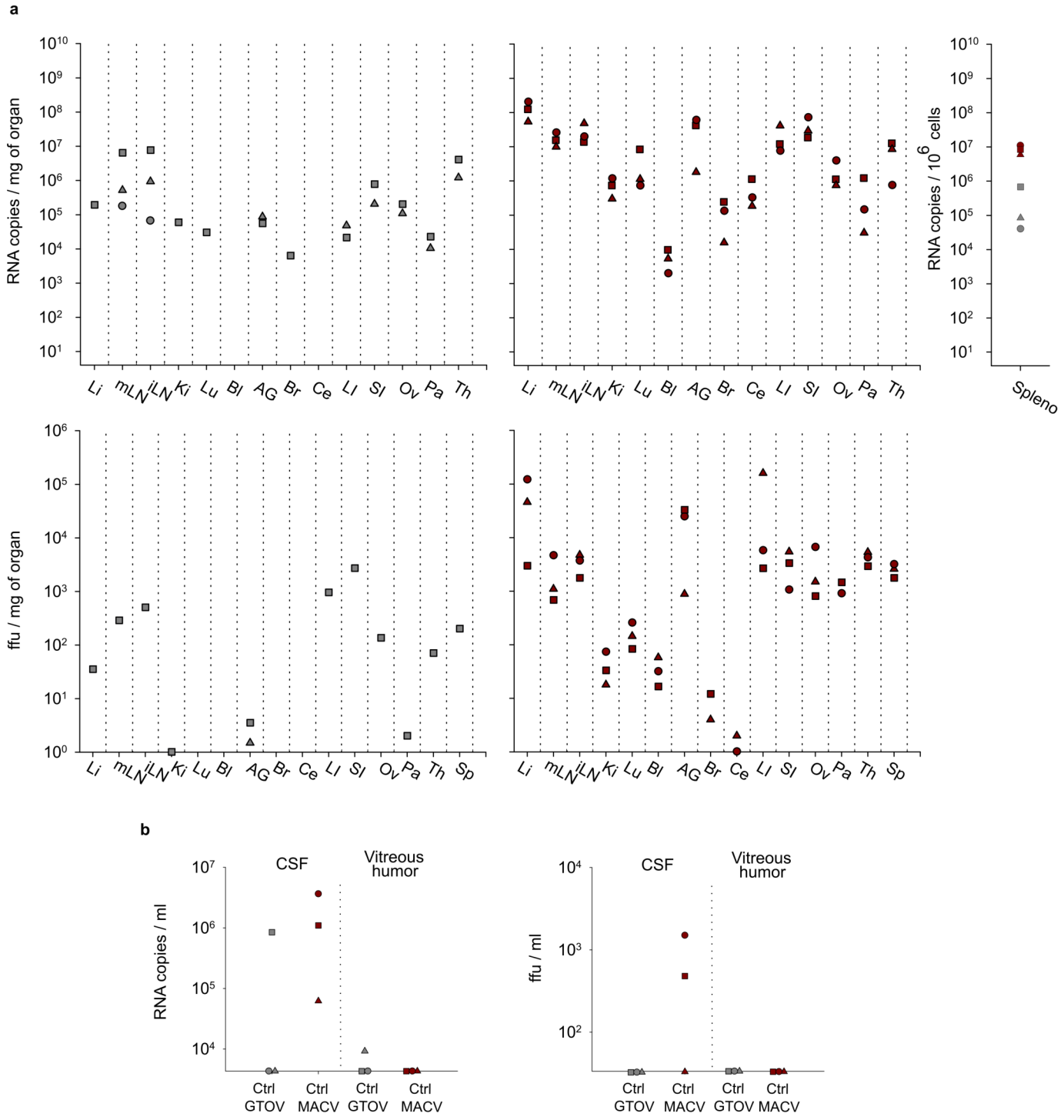

Extended Data Fig. 7

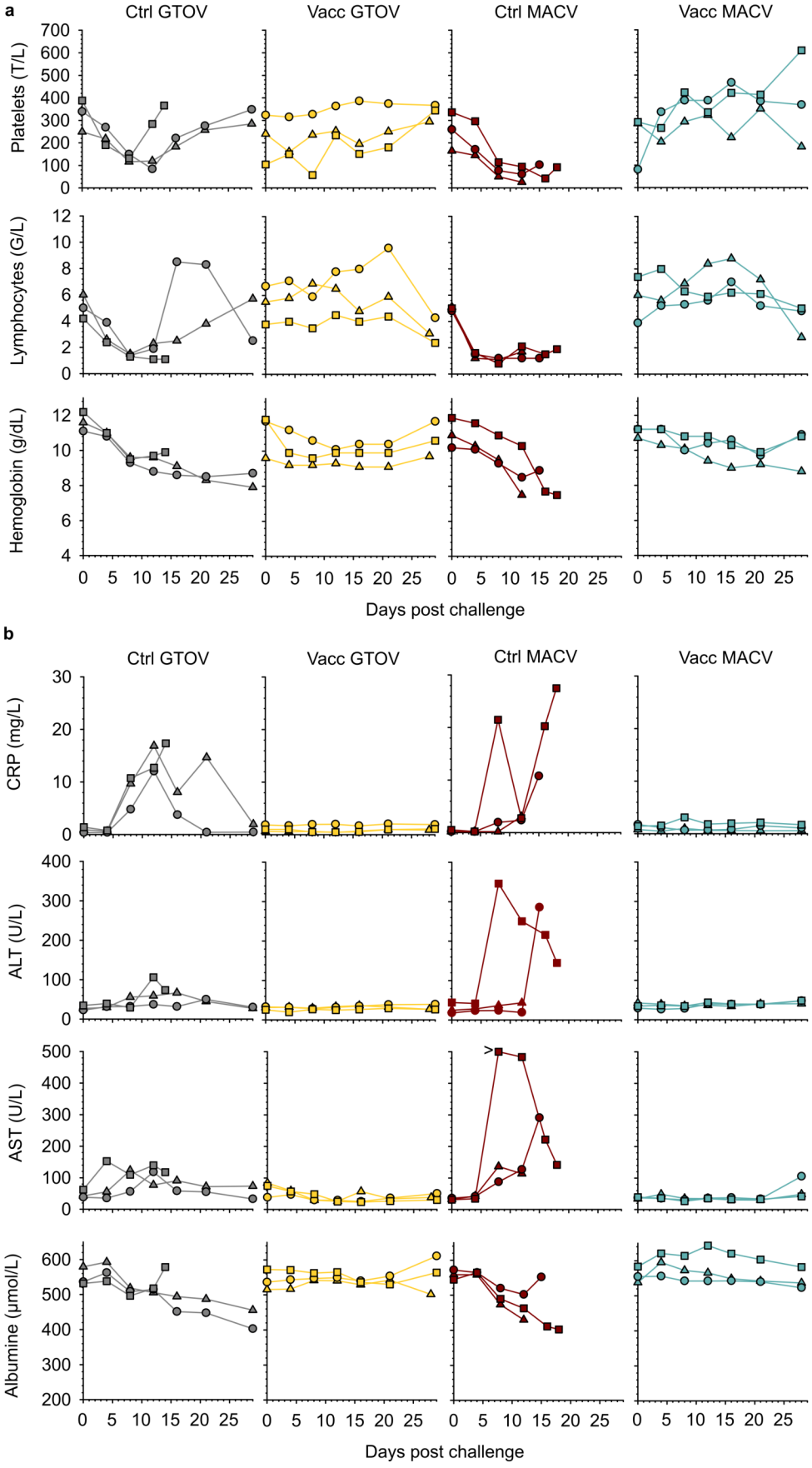

Extended Data Fig. 8

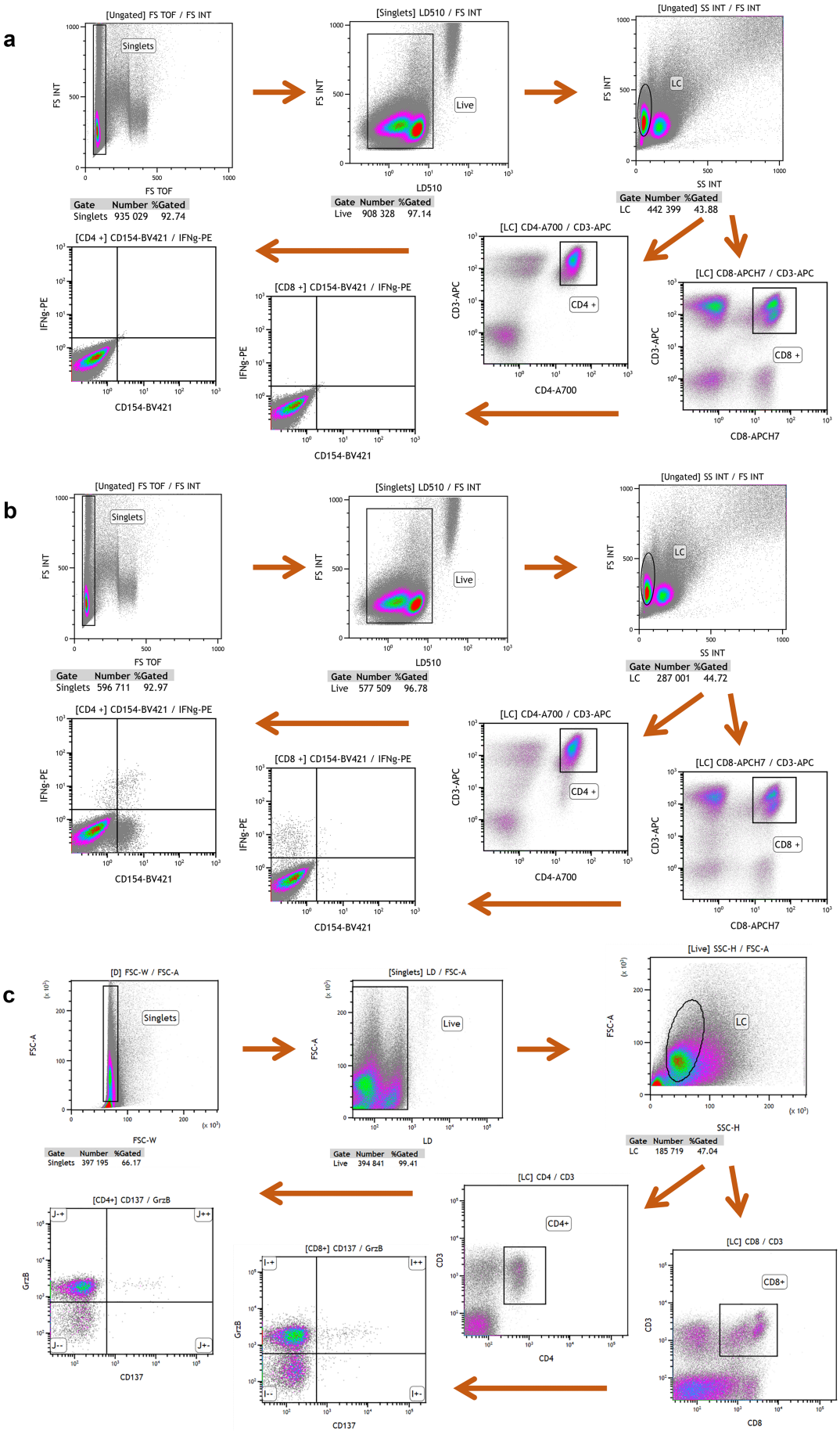

Extended Data Fig. 9